

**TURBULENT FLOW BEHAVIOUR OF NON-
NEWTONIAN FLUID IMPINGING JETS OVER
FLAT PLATES WITH PERIODIC HEAT FLUX
BOUNDARY CONDITION.**

A Thesis Submitted for Partial Fulfillment of the

Requirements for the Degree of

Master of Engineering in Automobile Engineering

By

RAJAT KARN

[Examination Roll Number: M4AUT22007]

[Registration Number: 154340 of 2020-21]

under the Guidance of

Dr. SUDIP SIMLANDI and Dr. SANDIP SARKAR

Professor

Department of Mechanical Engineering

Faculty of Engineering and Technology

Jadavpur University

Kolkata-700032

Faculty of Engineering and Technology
Department of Mechanical Engineering
Jadavpur University
Kolkata-700032

**DECLARATION OF ORIGINALITY AND COMPLIANCE OF
ACADEMIC ETHICS**

I hereby declare that this thesis contains literature survey and original research work by the undersigned candidate, as part of his MASTER OF ENGINEERING IN AUTOMOBILE ENGINEERING studies. All information in this document have been obtained and presented in accordance with the academic rules and ethical conduct.

I also declare that as required by these rules and conduct, I have fully cited and referred all material and results that are not original to this work.

RAJAT KARN

Examination Roll Number: M4AUT22007

Registration Number: 154340 of 2020-21

**Thesis Title: Turbulent Flow Behaviour of Non Newtonian Fluid
Impinging Jets Over Flat Plates with periodic heat flux boundary
condition.**

Signature:
(Rajat Karn)

Dated:

Faculty of Engineering and Technology
Department of Mechanical Engineering
Jadavpur University
Kolkata-700032

Certificate of Approval*

*This forgoing thesis, entitled “ **Turbulent Flow Behaviour of Non Newtonian Fluid Impinging Jets Over Flat Plates with Periodic Heat Flux Boundary condition.**” is hereby approved as a credible study of an engineering subject carried out and presented in a manner satisfactory to warrant its acceptance as a prerequisite to the degree for which it has been submitted. It is understood that by this approval the undersigned do not endorse or approve any statement made, opinion expressed or conclusion drawn therein but approve the thesis only for the purpose of which it has been submitted.*

Committee on final examination for evaluation of the thesis

Signature:

Signature:

Date:

Date:

Seal:

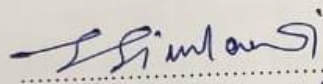
Seal:

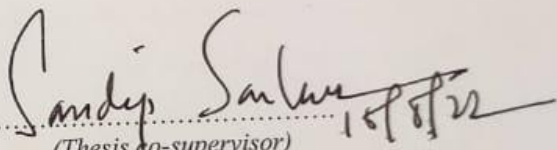
***Only in case, the thesis is approved.**

Faculty of Engineering and Technology
Department of Mechanical Engineering
Jadavpur University
Kolkata-700032

CERTIFICATE OF RECOMMENDATION

We hereby recommend that the thesis presented by Mr. Rajat Karn entitled "*Turbulent Flow Behaviour of Non Newtonian Fluid Impinging Jets Over Flat Plates with Periodic Heat Flux Boundary condition*", was under our supervision and is accepted in partial fulfilment of the degree of Master of Engineering in Automobile Engineering.


.....
(Thesis Supervisor) 16/08/2022
Dr. Sudip Simlandi
Professor
Department of Mechanical Engineering
Jadavpur University
Kolkata-700032

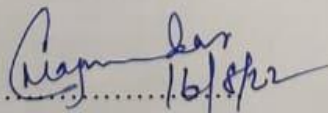

.....
(Thesis co-supervisor) 16/08/22
Dr. Sandip Sarkar
Professor
Department of Mechanical Engineering
Jadavpur University
Kolkata-700032

Countersigned by:


.....

(Head of the Department, Mechanical Engineering)

Date: Professor & Head
Dept. of Mechanical Engineering
Seal: Jadavpur University, Kolkata-32


.....

(Dean of Faculty of Engineering and Technology)

Date:
Seal:  **DEAN**
Faculty of Engineering & Technology
JADAVPUR UNIVERSITY
KOLKATA-700 032

Table of Contents

Acknowledgement	7
Abstract	8
List of Figures	9
Nomenclature	13
CHAPTER 1 Introduction	14
1.1 Fundamentals of Fluid:	15
1.2 Basics of Jet Impingement	16
1.3 Geometry of Jet:	17
CHAPTER 2 Literature Review	18
2.1 Literature Review	18
2.2 Summary of the Literature Review	21
2.3 Work plan for current study	22
CHAPTER 3 Simulation Model	23
3.1 Physical domain definition	23
3.2 Geometry of the simulation model	24
3.3 3D model mesh generation:	25
3.4 Simulation setup and Boundary conditions:	26
3.5 Governing Equations:	28
3.6 Grid independent test:	31
3.7 Validation 1 :	31
3.8 Validation 2 :	32
CHAPTER 4 Results and Discussions	34
4.1 Results obtained for inlet velocity of 0.5 m/s	34
4.1.1. Velocity contours	36
4.1.2. Velocity streamlines	38
4.1.3. Velocity vector	39
4.1.4. Temperature contours	40
4.1.5. Nusselt no. contour	42
4.1.6. Temperature vs x coordinate variation chart	43
4.1.7. Nusselt no. vs x coordinate variation chart	45
5. The Nusselt number observations:	47

6.2 Results obtained for inlet velocity of 1.5 m/s	49
6.2.1.Velocity contours.....	49
6.2.2 Velocity streamlines	51
6.2.3 Velocity vector	53
6.2.4 Temperature contour	55
6.2.5 Nusselt no. contour	57
6.2.6 Temperature vs x coordinate variation chart	59
6.2.7 Nusselt no. vs x coordinate variation chart	61
CHAPTER 5.....	63
5.1 Conclusion.....	63
5.2 Future scope of this study	64
REFERENCES :.....	65

ACKNOWLEDGEMENT

*I take this opportunity to express a deep sense of gratitude towards my guide **Dr. Sudip Simlandi**, Department of Mechanical Engineering ,for providing excellent guidance, encouragement and inspiration throughout the project work , which helped me a lot to improve this project work. I express my heartiest thanks to **Dr. Sandip Sarkar**, department of mechanical engineering, and all the faculty members of Automobile Engineering for providing support during this research work.*

Additionally, I want to express my gratitude for the wonderful cooperation of all the non-teaching personnel, my entire batch, my seniors, and all of my friends.

Last but not least, I want to express my sincere appreciation and sentiments for my family, who have continuously provided me with the drive, motivation, and determination to pursue my academic goals.

Date :

RAJAT KARN

Abstract

The current research uses numerical analysis to examine the behaviour of a non-Newtonian power law fluid used as an impinging jet across a square flat plate with a periodic heat flow. A time-dependent sinusoidal heat flux has been applied to the flat plate that is being impinged. The flow conditions of turbulence have been taken into consideration for the circular jets. The power-law constitutive model, which has been rendered as a 3D model using ANSYS FLUENT, is used to analyse the jet's non-Newtonian behaviour. Fluids with Power-law indices (n) ranging from 0.6 to 1.6 have been employed, including pseudoplastic, Newtonian, and dilatant fluids.

SST- ($k-\omega$) model that comprises the continuity equation and the energy equation is used to describe turbulence. For velocities of $v = 0.5$ m/s or 1.5 m/s, the intake circumstances were changed, and corresponding values for such Nusselt number and the average temperature of the flat plate impinged were discovered. As a result, it was possible to evaluate the cooling effectiveness of various fluids utilised for jet impingement. According to the findings, cooling capacity decreased as the power law index rose. The cooling effect and capacity fluctuation of various fluids are shown by the Nusselt number and temperature distribution along the flat plate.

The non dimensional results obtained from the simulation of the 3D model were compared with the available standard data from the literature .

Keywords: Sinusoidal Heat flux, Power law fluid, Numerical Simulation, Turbulent, Impinging jet, Flat Plate.

List of Figures

Figure 1 A hot flat plate is shown, which is being cooled using jet impingement(google)	14
Figure 2 Various impingement jet flow regions.	16
Figure 3 The circular hydraulic jump.	17
Figure 4 Schematic 3D diagram of model with inlet, outlet and wall condition	23
Figure 5 2-D schematic diagram of the model	24
Figure 6 (a) side view and (b) front view of the geometry	25
Figure 7 isometric view of the geometry	25
Figure 8 Mesh generated for 3D model	26
Figure 9 Refined Mesh generated for face of the heated wall plate	26
Figure 10 Sinusoidal variation of heat flux with time	28
Figure 11 Average Nusselt no. Vs Power-law index 'n' for this study	32
Figure 12 Average Nusselt no Vs power-law index 'n' in literature.....	32
Figure 13 Dimensionless plot of Nu vs X in this study for n=0.8 V= 1.5 m/s.	33
Figure 14 Variation of Nu vs X present in literature [15]	33
Figure 15 velocity contour for n=0.6,v=0.5m/s	36
Figure 16 velocity contour for n=0.8,v=0.5m/s	36
Figure 17 velocity contour for n=1.0, v=0.5m/s.....	36
Figure 18 velocity contour for n=1.2, v=0.5m/s.....	36
Figure 19 velocity contour for n=1.4, v=0.5m/s.....	37
Figure 20 velocity contour for n=1.6, v=0.5m/s.....	37
Figure 21 velocity streamline for n=0.6, v=0.5m/s.	38
Figure 22 velocity streamline for n=0.8, v=0.5m/s.	38
Figure 23 velocity streamline for n=1.0, v=0.5m/s.	38
Figure 24 velocity streamline for n=1.2, v=0.5m/s.	38
Figure 25 velocity streamline for n=1.4, v=0.5m/s.	38
Figure 26 velocity streamline for n=1.6, v=0.5m/s.	38
Figure 27 velocity vector for n=0.6, v=0.5m/s.	39
Figure 28 velocity vector for n=0.8, v=0.5m/s.	39
Figure 29 velocity vector for n=1.0, v=0.5m/s.	39
Figure 30 velocity vector for n=1.2, v=0.5m/s.	39
Figure 31 velocity vector for n=1.4, v=0.5m/s.	39
Figure 32 velocity vector for n=1.6, v=0.5m/s.	39

Figure 33 Temperature contour for $n=0.6, v=0.5\text{m/s}$	40
Figure 34 Temperature contour for $n=0.8, v=0.5\text{m/s}$	40
Figure 35 Temperature contour for $n=1.0, v=0.5\text{m/s}$	41
Figure 36 temperature contour for $n=1.2, v=0.5\text{m/s}$	41
Figure 37 temperature contour for $n=1.4, v=0.5\text{m/s}$	41
Figure 38 temperature contour for $n=1.6, v=0.5\text{m/s}$	41
Figure 39 Nusselt no. contour for $n=0.6, v=0.5\text{m/s}$	42
Figure 40 Nusselt no. contour for $n=0.8, v=0.5\text{m/s}$	42
Figure 41 Nusselt no. contour for $n=1.0, v=0.5\text{m/s}$	42
Figure 42 Nusselt no. contour for $n=1.2, v=0.5\text{m/s}$	42
Figure 43 Nusselt no. contour for $n=1.4, v=0.5\text{m/s}$	42
Figure 44 Nusselt no. contour for $n=1.6, v=0.5\text{m/s}$	42
Figure 45 Temperature variation along line, for $n=0.6, v=0.5\text{m/s}$	43
Figure 46 Temperature variation along line, for $n=0.8, v=0.5\text{m/s}$	43
Figure 47 Temperature variation along line, for $n=1.0, v=0.5\text{m/s}$	43
Figure 48 Temperature variation along line, for $n=1.2, v=0.5\text{m/s}$	44
Figure 49 Temperature variation along line, for $n=1.4, v=0.5\text{m/s}$	44
Figure 50 Temperature variation along line, for $n=1.6, v=0.5\text{m/s}$	44
Figure 51 Nusselt no. variation along line, for $n=0.6, v=0.5\text{m/s}$	45
Figure 52 Nusselt no. variation along line, for $n=0.8, v=0.5\text{m/s}$	45
Figure 53 Nusselt no. variation along line, for $n=1.0, v=0.5\text{m/s}$	45
Figure 54 Nusselt no. variation along line, for $n=1.2, v=0.5\text{m/s}$	46
Figure 55 Nusselt no. variation along line, for $n=1.4, v=0.5\text{m/s}$	46
Figure 56 Nusselt no. variation along line, for $n=1.6, v=0.5\text{m/s}$	46
Figure 57 Nusselt number variation with dimensionless position for $v= 1.5 \text{ m/s}$	47
Figure 58 Variation of Nu with the dimensionless lateral position for $V=1.5 \text{ m/s}$	48
Figure 59 velocity contour for $n=0.6, v=1.5\text{m/s}$	49
Figure 60 velocity contour for $n=0.8, v=1.5\text{m/s}$	49
Figure 61 velocity contour for $n=1.0, v=1.5\text{m/s}$	49
Figure 62 velocity contour for $n=1.2, v=1.5\text{m/s}$	50
Figure 63 velocity contour for $n=1.4, v=1.5\text{m/s}$	50
Figure 64 velocity contour for $n=1.6, v=1.5\text{m/s}$	50
Figure 65 velocity streamline for $n=0.6, v=1.5\text{m/s}$	51
Figure 66 velocity streamline for $n=0.8, v=1.5\text{m/s}$	51

Figure 67 velocity streamline for $n=1.0, v=1.5\text{m/s}$	51
Figure 68 velocity streamline for $n=1.2, v=1.5\text{m/s}$	52
Figure 69 velocity streamline for $n=1.4, v=1.5\text{m/s}$	52
Figure 70 velocity streamline for $n=1.6, v=1.5\text{m/s}$	52
Figure 71 velocity vector for $n=0.6, v=1.5\text{m/s}$	53
Figure 72 velocity vector for $n=0.8, v=1.5\text{m/s}$	53
Figure 73 velocity vector for $n=1.0, v=1.5\text{m/s}$	53
Figure 74 velocity vector for $n=1.2, v=1.5\text{m/s}$	54
Figure 75 velocity vector for $n=1.4, v=1.5\text{m/s}$	54
Figure 76 velocity vector for $n=1.6, v=1.5\text{m/s}$	54
Figure 77 Temperature contour for $n=0.6, v=1.5\text{m/s}$	55
Figure 78 Temperature contour for $n=0.8, v=1.5\text{m/s}$	55
Figure 79 Temperature contour for $n=1.0, v=1.5\text{m/s}$	55
Figure 80 Temperature contour for $n=1.2, v=1.5\text{m/s}$	56
Figure 81 Temperature contour for $n=1.4, v=1.5\text{m/s}$	56
Figure 82 Temperature contour for $n=1.6, v=1.5\text{m/s}$	56
Figure 83 Nusselt no. for $n=0.6, v=1.5\text{m/s}$	57
Figure 84 Nusselt no. for $n=0.8, v=1.5\text{m/s}$	57
Figure 85 Nusselt no. for $n=1.0, v=1.5\text{m/s}$	57
Figure 86 Nusselt no. for $n=1.2, v=1.5\text{m/s}$	58
Figure 87 Nusselt no. for $n=1.4, v=1.5\text{m/s}$	58
Figure 88 Nusselt no. for $n=1.6, v=1.5\text{m/s}$	58
Figure 89 Temperature variation along line, for $n=0.6, v=1.5\text{m/s}$	59
Figure 90 Temperature variation along line, for $n=0.8, v=1.5\text{m/s}$	59
Figure 91 Temperature variation along line, for $n=1.0, v=1.5\text{m/s}$	59
Figure 92 Temperature variation along line, for $n=1.2, v=1.5\text{m/s}$	60
Figure 93 Temperature variation along line, for $n=1.4, v=1.5\text{m/s}$	60
Figure 94 Temperature variation along line, for $n=1.6, v=1.5\text{m/s}$	60
Figure 95 Nusselt no. variation along line, for $n=0.6, v=1.5\text{m/s}$	61
Figure 96 Nusselt no. variation along line, for $n=0.8, v=1.5\text{m/s}$	61
Figure 97 Nusselt no. variation along line, for $n=1.0, v=1.5\text{m/s}$	61
Figure 98 Nusselt no. variation along line, for $n=1.2, v=1.5\text{m/s}$	62
Figure 99 Nusselt no. variation along line, for $n=1.4, v=1.5\text{m/s}$	62
Figure 100 Nusselt no. variation along line, for $n=1.6, v=1.5\text{m/s}$	62

List of Tables

Table 1 Mesh parameters	25
Table 2 Properties of the impinged fluid	27
Table 3 Properties of the solid plate	27
Table 4 Grid independence test	31

Nomenclature

<i>Symbol</i>	<i>Description</i>	<i>SI units</i>
x	Co-ordinates parallel to the plate	[mm]
y	Co-ordinates normal to the plate	[mm]
Nu	Based on the diameter of nozzle diameter, Nusselt number.	[-]
Q	Heat flux.	[W/m ²]
h	heat transfer coefficient	[W.m ⁻² .K ⁻¹]
H	Distance between inlet of jet and the target plate.	[mm]
k	Thermal Conductivity of the fluids used	[W.m ⁻¹ .k ⁻¹]
K	Kelvin Temperature Scale.	[K]
L	Model's Length .	[mm]
n	Fluid's Power law Index.	[-]
Re	Reynolds number.	[-]
T	Plate Temperature	[K]
T_j	Jet Temperature	[K]
T_l	Local temperature of plate.	[K]
V	Jet Velocity	[m/s]
W	Width of the jet	[mm]

Greek Symbols

ρ	Density of the fluid	[kg/m ³]
φ	Shear strain rate	[1/s]
μ	Viscosity of the jet	[kg m ⁻¹ s ⁻¹]
κ	Flow consistency index of jet	[-]

Subscripts

avg	Average
-------	---------

1

Introduction

When high heat transfer rates are necessary, impingement of the jet is crucial in many industrial and technical applications. In numerous prime industries like manufacturing industries, cooling and quenching processes which require quick, efficient and controlled cooling of the specimen, cooling of electronic devices such as processors within a compact geometrical design, controlled cooling of high performance computer components, cooling of gas turbine blades, localized cooling in internal combustion engines, cooling processes in paper industries, food and textile products, etc., implementation of jet impingement is required. As the temperatures of these metal specimens and machinery parts can be very high (of the order 800-1200 °C), having a uniform heat flux or it can be localised heating, especially for electronic and mechanical systems. Either of the gaseous and liquid media can be implied depending on various parameters and requirements, like the temperature, heat flux, and optimum effectiveness of cooling.

Due to abundant and ease in availability, air has readily been used as a working medium for jet impingement and a numerous research on impinging air jets [1,2] has already been performed. But, recent studies showing the comparison of gaseous jets and liquid jets have drawn more attention to the study of liquid jets, as liquid jets show enhanced heat transfer rates of several higher orders.

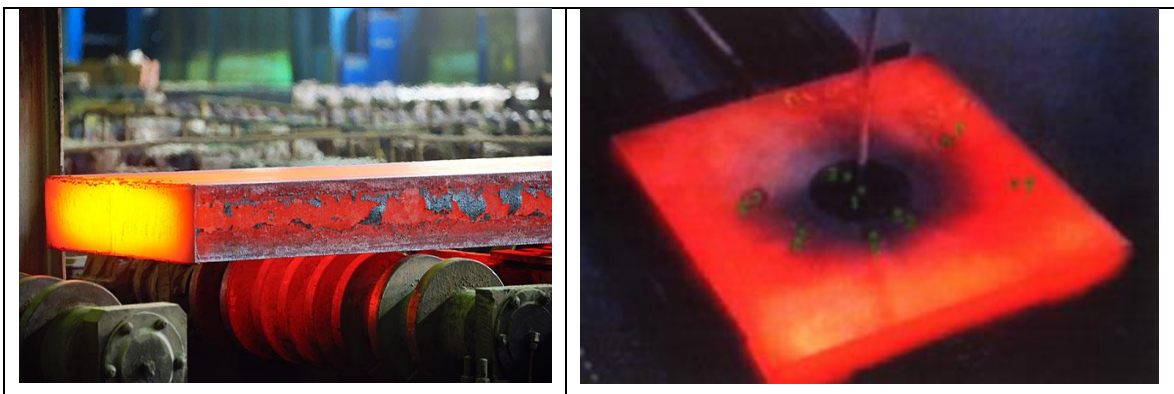


Figure 1 A hot flat plate is shown, which is being cooled using jet impingement. (google)

1.1 FUNDAMENTALS OF FLUID:

Fluid can be defined as a substance that deforms continuously when a shear force is applied, irrespective of the magnitude of applied tangential force, a fluid at rest can't withstand a shear stress it'll start deforming. The delivered shear stress in fluids is thus exactly proportional to the strain rate.

Fluids are typically divided into two categories depending on their properties: Newtonian fluids and Non-Newtonian fluids.

Newton's laws of viscosity, which can be stated as, are observed by Newtonian fluids.:

$$\tau = \mu \frac{du}{dy} \quad (1)$$

where, μ = dynamic viscosity,

τ = shear stress,

$\frac{du}{dy}$ = strain rate or the velocity gradient of the fluid.

Non-Newtonian power law model defines Non-Newtonian fluids by raising the power of shear strain to 'n', thus changing the properties of fluid as:

$$\tau = \mu \left(\frac{du}{dy} \right)^n \quad (2)$$

where, n is called as the power law index.

Non-Newtonian fluids exhibit an apparent viscosity rather than the property of viscosity, that may be calculated as such ratio of the local shear stress to the shear rate at that location. Its significance is influenced by the flow field as well as shear rate.

Depending on the value of 'n', the non-Newtonian fluid which are time independent, can further be classified into:

- (a) Pseudoplastic Fluid (or shear thinning), for 'n' < 1, examples: Milk, Blood, Gelatine, etc.
- (b) Dilatant (or shear thickening), for 'n' > 1, examples : Sugar solution, high concentration sand suspension , Starch suspension etc.
- (c) Bingham plastic: fluids which require an initial yield stress in order to establish the flow, 'n' = 1, but initial stress is present.

Time dependent Non-Newtonian fluids having values $n > 1$ and $n < 1$ are known as rheopectic and thixotropic fluids.

In this study, time independent Non-Newtonian fluids have been compare with Newtonian fluids.

1.2 BASICS OF JET IMPINGEMENT

Convective heat transmission from a flat surface is triggered by the fine layer that develops if a liquid jet impacts it and radiates radially away from the spot of impact.

A Jet impingement flow can be seen in the fig 2, where different flow regions are shown.

The Jet impingement flow can be subdivided into following regions:

- *The stagnation zone.*
- *The boundary layer region.* The viscous boundary layer thickness in this region is less than the liquid sheet thickness, also the liquid on the surface is unaffected by the wall friction.
- *The fully viscous sheet.* Here, the boundary layer thickness is same as the sheet thickness. The viscous influence extends through the entire liquid film, from the wall to the free surface.
- *The hydraulic jump.* In this region, an abrupt increase of liquid sheet thickness can be seen and the velocity of impinged fluid is much lower comparing to that in the upstream region.

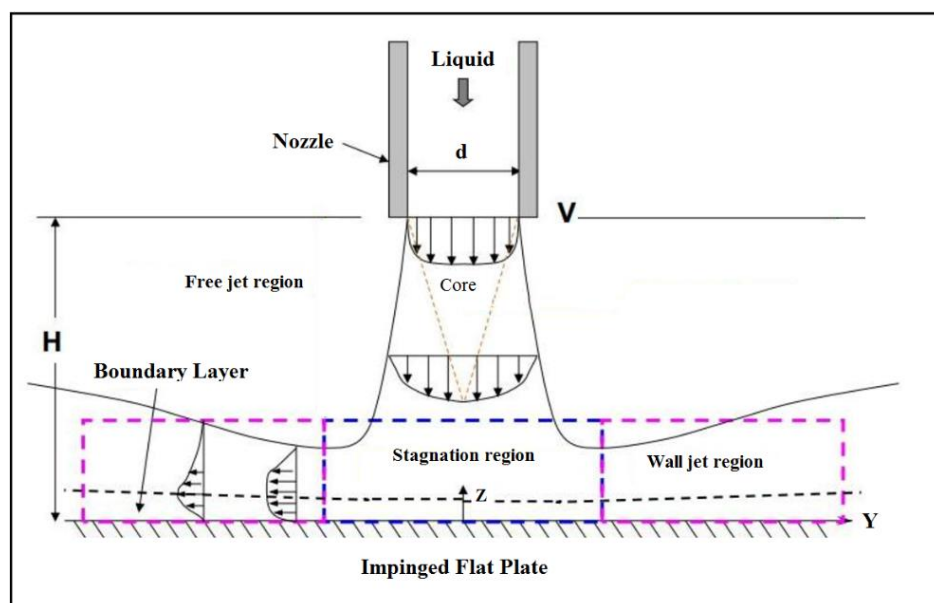


Figure 2 Various impingement jet flow regions.

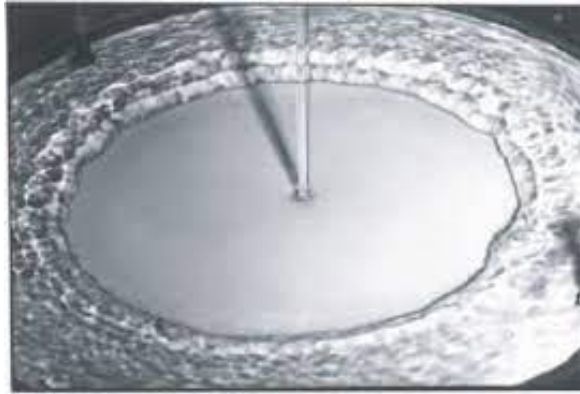


Figure 3 The circular hydraulic jump.

1.3 Geometry of Jet:

The structure of the jet on which the heat transfer happens is also determined by this. It can take on a variety of geometric shapes, and each shape affects the heat transmission qualities in a particular way. Typical forms for jet include: The fluid is discharged along the axis of the axial jet in axial jets with a circular nozzle or from a tube. A rectangular nozzle used in the Slot or planar jets releases the fluid. Not in a radial fashion. The fluids in the radial jets, which are formed after impact, spread mostly in this direction.

In this study a circular jet has been implied on the flat plate.

Literature Review

2.1 Literature Review

In this section, literature surveys related to jet impingement studies which have been carried out has been discussed. The studies where a free jet strikes the surface from the top. Based on the type of jet impingement, steady and transient jets have been discussed.

- **R. Gharraei and A. Vejdani et al. [1]** conducted a numerical research for numerous square jets impinging on a plate, where the Nusselt number, jet-to-plate separation, and impact of the fluids' power law indices on the flow structure were examined. According to the findings, a decrease in jet-to-plate separation causes an increase in the wall Nusselt number. It also came to the conclusion that an increase in the power-law index for a given Reynolds number and a constant consistency coefficient indicates a higher impingement velocity, which leads to an increase in the wall Nusselt number. Peripheral entrainment vortices are formed surrounding the jet body for higher jet-to-plate separation values, and the vortices vanished if the distance was reduced.
- **Allauddin, N. Uddin, and B. Weigand [2]** studied the jet impingement on axisymmetric detached ribs heat transfer augmentation on a flat surface. For both cases of a single and a multiple jet, having a crossflow interaction has been investigated. The influence of high values of jet Reynolds number ranging from 7000 to 78,000, with a blowing ratio ranging between 5.8 and 11.5, the ratio of height of impingement to the diameter of the jet ranging between 2 to 6 has been examined. Results showed that the heat transfer enhances on the target surface, having detached ribs in the case of single as well as for multiple jet impingement at a moderate crossflow speed.
- **J. S. Ten and T. Povey [3]** studied the pulsed impinging jet for gas turbine cooling, where jet is self exciting, aiming to enhance the heat transfer rate.

Simulations were done for Self- excited oscillatory behavior of jet, and results were obtained for a wide range of inlet to outlet pressure ratios. It was found that due to extreme pressure loss inside the device, the resulting heat transfer rate was not enhanced but varied greatly in comparison to that of the ideal conditions.

- **Chen et al.** [4] performed a theoretical study of jet impingement heat transfer analysis with single phase, free surface slot jet. Arbitrary-heat-flux conditions were used. The general expressions of heat transfer coefficients were obtained from the various regions of flow along the stagnation zone and three defined wall jet zones. The investigation of laminar flow and the developed equations to describe the local heat-transfer coefficients were done.
- **M. Behnia et al.** [5] studied the numerical prediction of turbulent impinging jet flows. Important parameters which determines the accuracy of a numerical predictions. It emphasised on the role and impact of the applied boundary conditions in a simulation. Here, an Axisymmetric round jet impinging normally and impinging at an angle to the target flat surface, with varying distances of impingement were shown. Results of this study highlights modelling issues regarding the entrainment, streamline curvature and heat transfer characteristics specially in the stagnation region of flow.
- **Gus Nasif, Ron Barron and Ram Balachandar** [6] studied the thermal characteristics of an oil jet which was impinged on a stationary flat disc having a uniform heat flux being settled in a confined space. The heat transfer coefficient was determined along with the effect of dimension of nozzle on the thermal characteristics were also investigated. The results shown that for jets being longer in length which are impinging on a stationary boundary, the geometry of nozzle has no significant effect on the studied thermal characteristics.
- **Fuchang Xu, Mohamed S. Gadala** [7] determined the heat fluxes for hot flat plates being cooled by water jet impingement at industrial scale test facility. According to the study's findings, the water temperature has a greater impact on heat transfer performance at stagnation than water flow rate, with the plate's steel grade having a less significant influence.
- **Md A. Teamah et al.** [8] used the oblique jet to study the hydrodynamic flow structure having a unique non circular profile. The nozzle inclination was varied from 30 to 90 degrees and jet flow rate was varied from 2 to 5lpm to get the

different results and circular hydraulic jump was obtained whereas an elliptical shape of hydraulic profile was obtained for oblique jet.

- **A. Bolek and S. Bayraktar [9]** determined the flow and the heat transfer characteristics of an impinging jet having a circular cross-sectional, being issued from a circular pipe impinging on the target plates which are having rectangular, convex and concave hemispherical shapes. The numerical investigation was done by varying the Reynolds numbers and jet-to-plate distances for all three cases. The results shown the regions where maximum heat transfer was obtained for rectangular plate. Also concluded that convex surface provided maximum but the concave surface had the minimum heat transfer. It was also observed that the Nusselt number increased with Reynolds number for concave and convex surface.
- **K Marzec and A Kucaba-Pietal[10]** used different nozzle geometries with multi jet impingement on flat plate, where inline array of six jets were used. The results shown that the values of heat transfer coefficient and the Nusselt number were different when different types of nozzles which are used. The study focused on the pressure drop and mass flow distribution for each type of nozzle. The chamfer nozzle's initial jet in the array had the largest deflection angle, which was observed. Lowest pressure drop for countersunk nozzles was achieved during analysis.
- **B. Sagot et al.[11]** conducted an experimental investigation for the round jet impingement on a flat plate having a constant wall temperature. Average Nusselt number correlation was determined. The result shown that for constant wall temperature, average Nusselt number is lower than that for a wall having constant heat flux.
- **A. M. Tahsini, and S. Tadayon Mousavi [12]** studied the confined turbulent slot jet impingement on flat plate. Where the effects of turbulent intensity of nozzle, effect of height of impinging jets were studied with constant value of Reynold's number. The effect of compressibility for confined jet was studied when Mach number was varied keeping a constant value of Reynold's number.
- **X. Liu and J.H. Leinhard [13]** studied a subcooled water jet impingement on plate having a uniform flux. The radial temperature distribution and the local Nusselt number variations were shown as a function of the Reynolds number.

- **Sheng et al. [14]** investigated the transient heat transfer for 2D annular fins of various geometrical shapes, having a sinusoidal heat flux varying with time. The transient heat conduction in for both a long slab and a long cylinder was studied using an improved lumped parameter model. The slab and tube geometry's transient temperature distribution was predicted. The border heat flow and heat generation in both the slab and the tube were measured for various scenarios and analysed. Additionally, a variety of temperature profiles were employed to find the slab's solution. One such results of the study conducted the amended Biot number. The findings demonstrated that the Biot number, which was a important factor in the heat transfer processes in solids, was really a factor of the modified Biot number.

2.2 Summary of the Literature Review

The following observations were made while studying the literature survey:

- Liquid jet impingement has enhanced heat transfer capabilities than that for gas jet.
- For long jets being impinged on a stationary boundary, the geometry of the nozzle has no significant effect on the thermal characteristics.
- The heat transfer behaviour at the stagnation region is mainly affected by the inlet fluid temperature and hardly affected by the fluid flow rate.
- Impinged plate having convex surface provided maximum and the concave surface had the minimum transfer of heat respectively. For surfaces that are concave or convex, Nusselt number grew as Reynolds number did.
- The value of Heat Transfer coefficient, depends on the geometry of nozzle. Countersunk type of nozzles has lowest pressure drop, whereas for chamfer nozzle high pressure drop was observed.
- For constant wall temperature, average Nusselt number is lower than that for a wall having constant heat flux.
 - Given Reynold's number and flow consistency index, for continuous heat flux. Peripheral entrainment vortices form surrounding the jet body for greater jet-to-plate spacing, and by reducing the distance, these vortices dissipated.

2.3 Work plan for current study

The present study emphasizes on the heat transfer characteristics and parameters affecting the cooling of a square flat plate with periodic heat flux. The implied heat flux is sinusoidal in nature. The impinged jets are power-law fluids with varying power law indices in the range of 0.6 to 1.6. The impingement jet velocities have been varied for values of $v = 0.5$ m/s and $v = 1.5$ m/s. The results are to be compared with the Newtonian fluids. A simulation model in the 3D domain has to be analysed. The turbulent behaviour of the impinged jet implied with the SST- $k\omega$ model is used for turbulent thermo-fluidic transport characteristics of the impinging jet.

In the present study, following observations are to be determined for different velocities:

- Study the nature of velocity streamlines and contours of the impinged jet.
- Nusselt number variation along the flat plate which will provide heat transfer characteristics.
- Temperature variation along the flat plate and effect of velocities to be determined.

Simulation Model

3.1 Physical domain definition

In this study, a circular non-Newtonian jet is impinged on a square flat plate which is having a periodic heat flux. The model for the impinged jet used is a long cylindrical pipe of constant diameter entering the region of our interest. The present investigation deals with the 3D simulation of the impingement process. The inlet and pressure outlet directions are shown in the Fig.4.

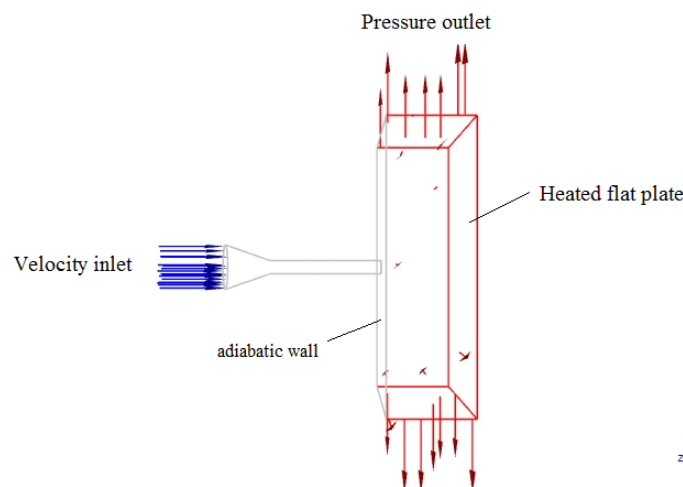


Figure 4 Schematic 3D diagram of model with inlet, outlet and wall condition

Figure 5 also depicts a 2-D domain where a steady jet with a defined inlet velocity, emerging from a defined nozzle of diameter(d), strikes a heated flat plate that is receiving a sinusoidal heat flux. The inlet jet temperature is 300K. H is the height of impingement, which is the height defined between the jet and the target flat heated surface (it has been defined as $L/3$ for this study and this value has been kept constant), L is taken as a target flat plate length. The ratios of H/d and L/d have been set to 6 and 20, respectively, for further non-dimensional and numerical research.

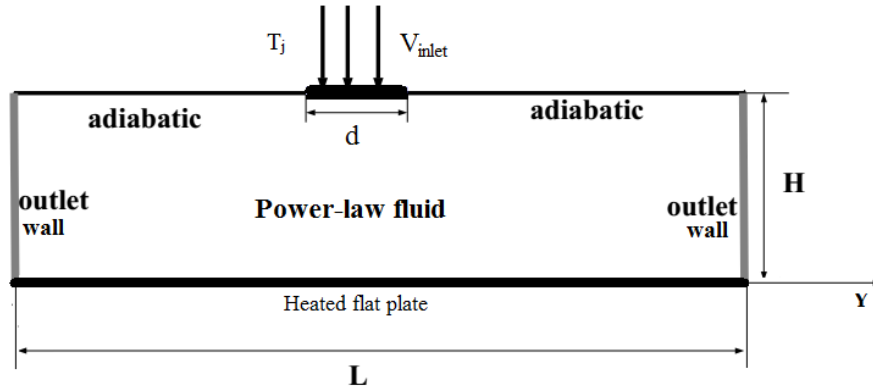


Figure 5 2-D schematic diagram of the model

For this inquiry, it has been presumed that the thermophysical qualities of the impinged non-Newtonian fluid remained constant and temperature invariant. As seen in Figure 5, the jet enters the enclosure at a height of $H=36$ mm, impinging on a wall 120 mm in length.

The flat wall is having a periodic heat flux, which is user defined function of a sinusoidal heat flux with time, with an amplitude of 1000.

The power-law index ‘ n ’, for the impinged non-Newtonian fluid has been varied for a range of $n=0.6-1.6$, for the jet inlet velocity $v = 0.5$ m/s and 1.5 m/s.

3.2 Geometry of the simulation model

The geometrical model is designed using Ansys 2022R1 fluent Design Modeler. As shown in the Fig 6(a), the right side view of the 3D model can be seen, which is the heated square wall plate, with no slip boundary condition. In the Fig 6(b), front view of the model can be seen, where circular jet has been generated while fluid flowing through a long cylindrical pipe, where the fluid is flowing in the $-z$ direction. In the Fig 6(c), isometric view of the model is shown, where the faces of the model is visible. The side walls of the model along with the walls adjacent to the incoming jet are stationary and having no slip boundary condition.

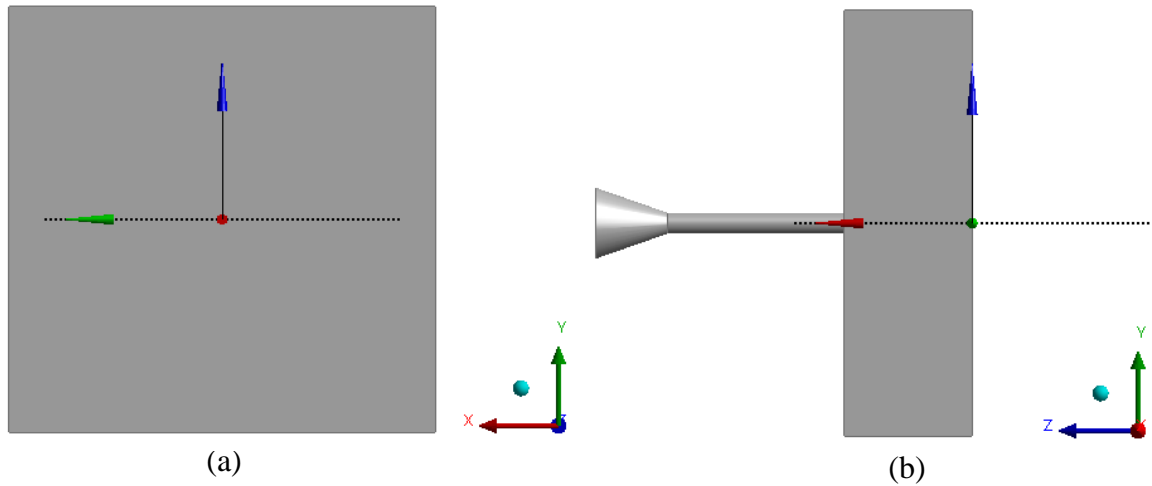


Figure 6 (a) side view and (b) front view of the geometry

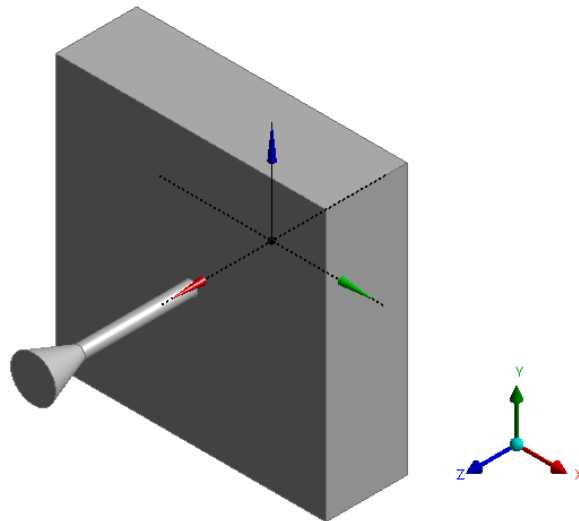


Figure 7 isometric view of the geometry

3.3 3D model mesh generation:

The Mesh has been generated for the 3D geometry for the jet as well as for the flat plate using Ansys Fluent. As the problem deals with the turbulent flow, fine mesh has been generated at the flat plate,(as this is the face where impingement regions and heat transfer processes occurs).Mesh parameters are listed in the Table 1.

Table 1 Mesh parameters

Type of mesh	No. of nodes	No. of cells	No. of faces	No. of elements
tetraheral	51113	226397	477840	226397

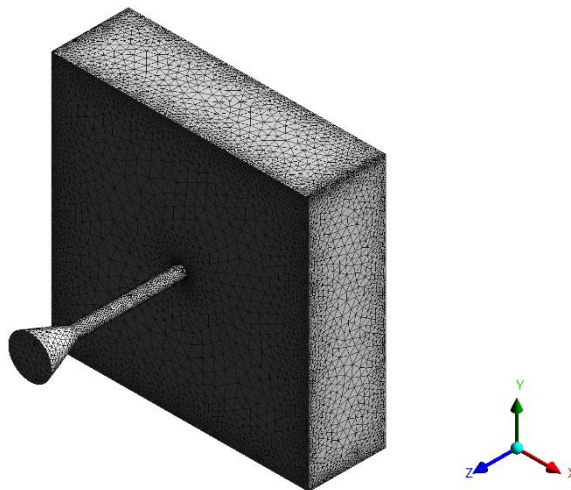


Figure 8 Mesh generated for 3D model

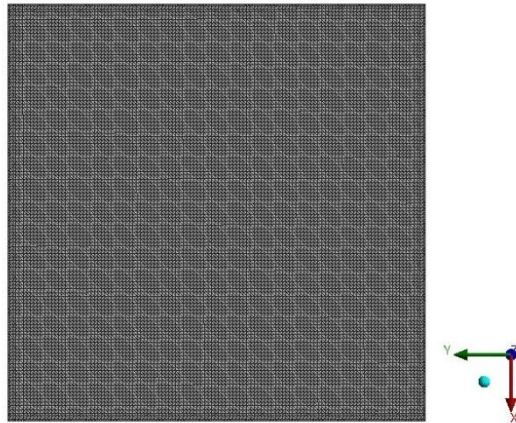


Figure 9 Refined Mesh generated for face of the heated wall plate

3.4 Simulation setup and Boundary conditions:

The simulation setup for the provided problem consists of the properties of the material used as solid, as well as the properties of the impinging jets, the models used for solving the numerical analysis, definition of the udf (user defined function) used along with the time specified of the impingement.

In this 3D simulation, SST k-omega turbulence model has been implied, with energy equation. The effect of gravity has not been considered, while unsteady conditions have been used. The heat flux function is sinusoidal, with a time period of 2π . The Non-Newtonian power law fluid has been used where power law index has been varied by 0.2, ranging from 0.6-1.6. The temperature of fluid is 300 K. The flow consistency index K has been considered to be constant for the complete analysis, as 0.01384. The properties of impinged

power-law fluid are shown in Table 2. An Aluminium plate has been used as impinged flat surface whose properties are enlisted in Table 3.

Table 2 Impinged fluid properties

Impinged Material	Density [kg/m ³]	Specific heat (J/kgK)	Thermal conductivity (W/m K)	Thermal Expansion coefficient	Viscosity (kg/m-s)	Power-law Index values
Non-Newtonian Fluid	998.2 (constant)	4182 (constant)	0.6 (constant)	0	variable	0.6, 0.8, 1.0, 1.2, 1.4, 1.6.

Table 3 Properties of the solid plate

Material	Density (kg/m ³)	Specific heat (J/kgK)	Thermal conductivity (W/mK)
Aluminium	2719	871	202.4

Boundary conditions :

- **Inlet conditions** : Velocity inlet condition has been used for the model. The analysis has been done for two velocities, with a resultant value of 0.5 m/s and 1.5 m/s. With 5% turbulence, the fluid is 300 K in temperature. The turbulent specification method used is “Intensity and Viscosity Ratio” and the turbulent viscosity ratio is 10.
- **Outlet conditions**: Pressure outlet is implied in this model. Walls are stationary with no slip conditions. Gauge pressure at outlet wall is 0, which implies that there is atmospheric pressure at the wall.
- **Flat plate wall conditions**: Material used for the model is Aluminium, having a heat flux thermal boundary condition. It is a stationary wall with no slip condition, the wall roughness constant is 0.5.
- The applied UDF for applied heat flux is sinusoidal in nature, varying with time along the wall plate, given by $1000 \cdot \sin(1 \cdot \text{time})$ with a time period of 6.283 seconds. The fluctuation in the heat flux over time is depicted in Figure 10.

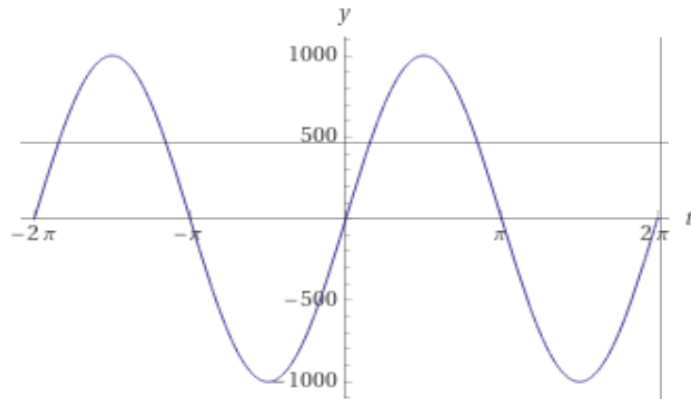


Figure 10 Sinusoidal variation of heat flux with time

Solution setup:

- The time step size used for simulation is 0.01 (s).
- Pressure, momentum, turbulent kinetic energy, specific dissipation rate, and energy are all calculated using the second order upwind method.
- The convergence criteria for the solution of velocity components in x, y, z directions, continuity and energy equations along with k and ω has been set for a value of 1e-6.

3.5 Governing Equations:

The governing equations used for the flow of non-Newtonian fluid used in this model are incompressible Navier-Stokes and energy equations, along with the turbulence, SST $k - \omega$ model has been used for the turbulence properties of the impinging jet. The SST $k - \omega$ model comprises of two-equations. These are two transport equations which are partial differential equation (PDEs), which accounts for the effects of convection processes and the diffusion of turbulent energy. The 2 transported variables enlisted are : (1) Turbulent kinetic energy (k), and (2). The specific turbulent dissipation rate (ω).

The turbulence kinetic energy (k) determines the energy in turbulence, and the specific turbulent dissipation rate (ω) determines the rate of dissipation per unit turbulent kinetic energy. The ω here, is also referred to as the scale of turbulence.

The governing equations used in dimensionless forms are:

Continuity equation:

$$\frac{\partial u_i}{\partial x_i} = 0 \tag{3}$$

Momentum equation:

$$\rho \frac{Du_i}{Dt} = -\frac{\partial p}{\partial x_i} + \frac{\partial \tau_{ij}}{\partial x_j} \quad (4)$$

Thermal energy equation:

$$\frac{DT}{Dt} = \alpha \frac{\partial^2 T}{\partial x_i \partial x_i} \quad (5)$$

In the above equations, u_i = velocity vector,

p = pressure,

T = fluid temperature,

ρ = density of the fluid

$\alpha = k/\rho C_p$ which is the thermal diffusivity.

k = thermal conductivity of the fluid

C_p = specific heat of fluid.

Neglecting the heat generating source term resulting from viscous dissipation.

Extra term τ_{ij} , for stress tensor is related to the deformation rate as :

$$\tau_{ij} = 2\lambda \varepsilon_{ij} \quad (6)$$

Where, ε_{ij} = deformation rate tensor.

The deformation rate tensor is also expressed as :

$$\varepsilon_{ij} = \frac{1}{2} \left(\frac{\partial u_i}{\partial x_j} + \frac{\partial u_j}{\partial x_i} \right) \quad (7)$$

Considering the model of non-Newtonian power law, where the second invariant of the deformation rate tensor affects the scalar viscosity function as :

$$\mu = \left(\frac{J_2}{2} \right)^{n-1/2} \quad (8)$$

Where ‘ n ’ = power-law flow behavioural index.

For , $n < 1$, shear-thinning behaviour of the fluid is observed,

$n > 1$, shear-thickening behaviour is observed,

and for $n = 1$, Newtonian behaviour is observed.

The second invariant of the deformation rate tensor J_2 , can be written as:

$$J_2 = \sum_i \sum_j \varepsilon_{ij} \cdot \varepsilon_{ji} \quad (9)$$

The standard $k-\omega$ model is a low Reynold’s number model, and it is generally used where the boundary layer is relatively thick and the viscous sublayer can be resolved.

Hence, the standard $k-\omega$ model suits best when required to be used for close wall problems.

Kinematic Eddy Viscosity:

$$\nu_T = \frac{a_1 k}{\max(a_1 \omega, S F_2)} \quad (10)$$

Turbulence Kinetic Energy :

$$\frac{\partial k}{\partial t} + U_j \frac{\partial k}{\partial x_j} = P_k - \beta^* k \omega + \frac{\partial}{\partial x_j} \left[(\nu + \sigma_k \nu_T) \frac{\partial k}{\partial x_j} \right] \quad (11)$$

Specific Dissipation Rate :

$$\frac{\partial \omega}{\partial t} + U_j \frac{\partial \omega}{\partial x_j} = \alpha S^2 - \beta \omega^2 + \frac{\partial}{\partial x_j} \left[(\nu + \sigma_\omega \nu_T) \frac{\partial \omega}{\partial x_j} \right] + 2(1 - F_1) \sigma_{\omega 2} \frac{1}{\omega} \frac{\partial k}{\partial x_i} \frac{\partial \omega}{\partial x_i} \quad (12)$$

The boundary conditions to solve the above-mentioned equations have been implied as discussed earlier in this section.

3.6 Grid independent test:

A grid independence study has been carried out for impinging non-Newtonian jet with power law index of 0.8 and inlet jet velocity of 0.5 m/s. Eight consecutive grids were examined for the mesh independency of this model. In Table 4, the corresponding values of the average Nusselt number on the flat plate are displayed. The Nusselt number of the wall plate was found to gradually vary when the mesh was polished and made finer. The observed percentage change in the average Nusselt no. for the sixth and seventh mesh sizes, however, is 2.37 percent, which is less than 3 percent. So, for better result along with optimum balance with computational time, mesh size with 51113 nodes having 226397 number of cells has been used.

Table 4 Grid independence test

Test	Number of nodes	Number of cells	Avg Nusselt number	% change
1	16212	75800	28.49	-
2	21925	101018	36.01	26.39
3	27177	124008	38.84	7.86
4	33158	149889	41.03	5.63
5	41768	186828	43.74	6.60
6	51113	226397	44.78	2.37
7	58081	255236	45.41	1.41
8	63969	279596	46.87	3.21

3.7 Validation 1 :

The obtained average Nusselt number vs power-law index 'n' plot have been shown for this study in the Fig 11. The values of Nusselt number were determined for both the velocities (0.5 m/s and 1.5 m/s). which is validated with the plot available in the literature for (jet impingement on flat plate having a constant flux) by V. Tiwari et.al [].as shown in fig 12.

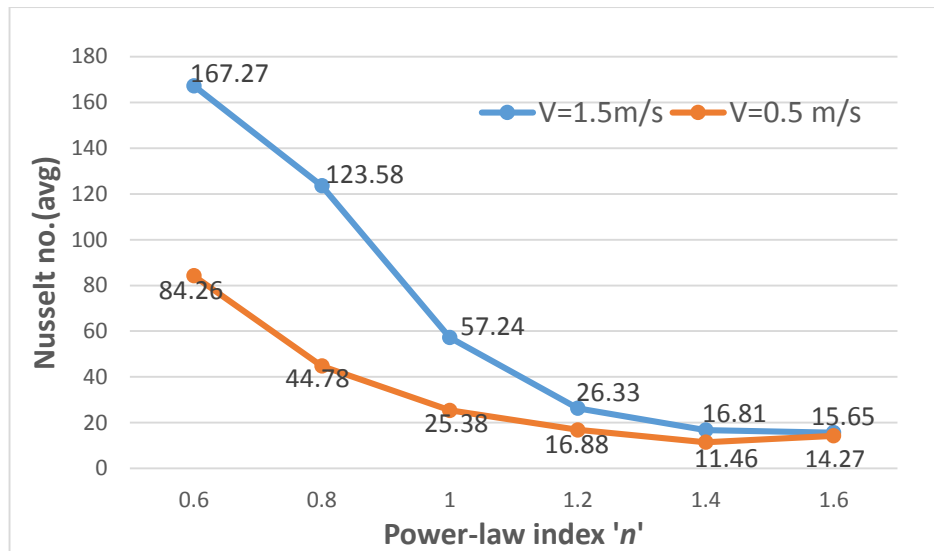


Figure 11 Average Nusselt no. Vs Power-law index 'n' for this study

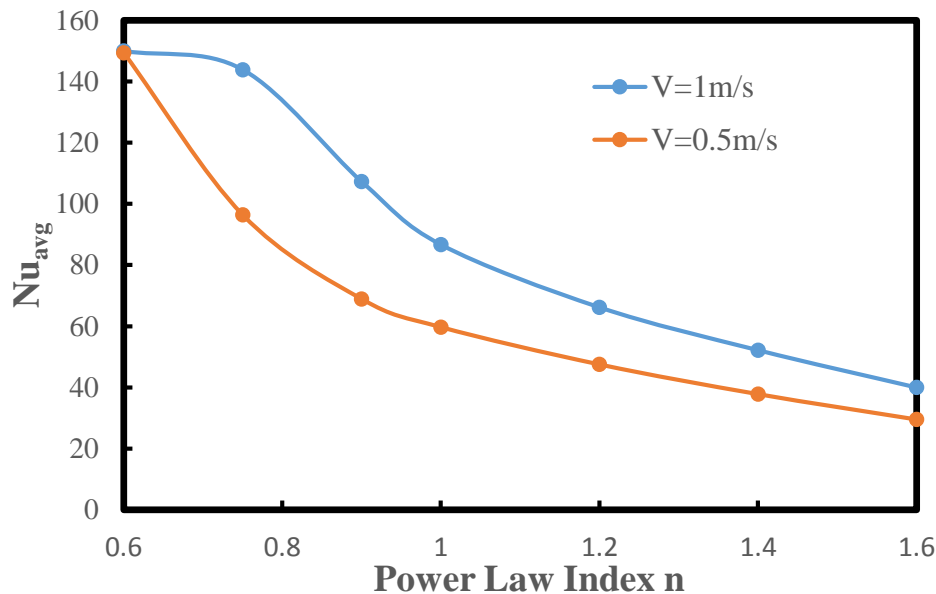


Figure 12 Average Nusselt no Vs power-law index 'n' in literature.

3.8 Validation 2 :

The generated result in my study have been shown in fig 13,for Nusselt number obtained about a line drawn along the heated wall plate, for impinged fluid with power law index of 0.8 and impinged velocity of 1.5 m/s. The H/d ratio used for this study is 6, hence the values obtained for Nusselt number varies from the literature, whereas the nature of variation of the Nusselt number is found similar to that of the variation discussed in the literature, [15](R.gharrei et al./International journal of thermal sciences 104 (2016)), where for low

Reynolds number, and $H/d = 1$, Nusselt number has been determined for impingement on flat plate. The Nusselt no variation with x axis along plate has been shown in fig 14, in literature.

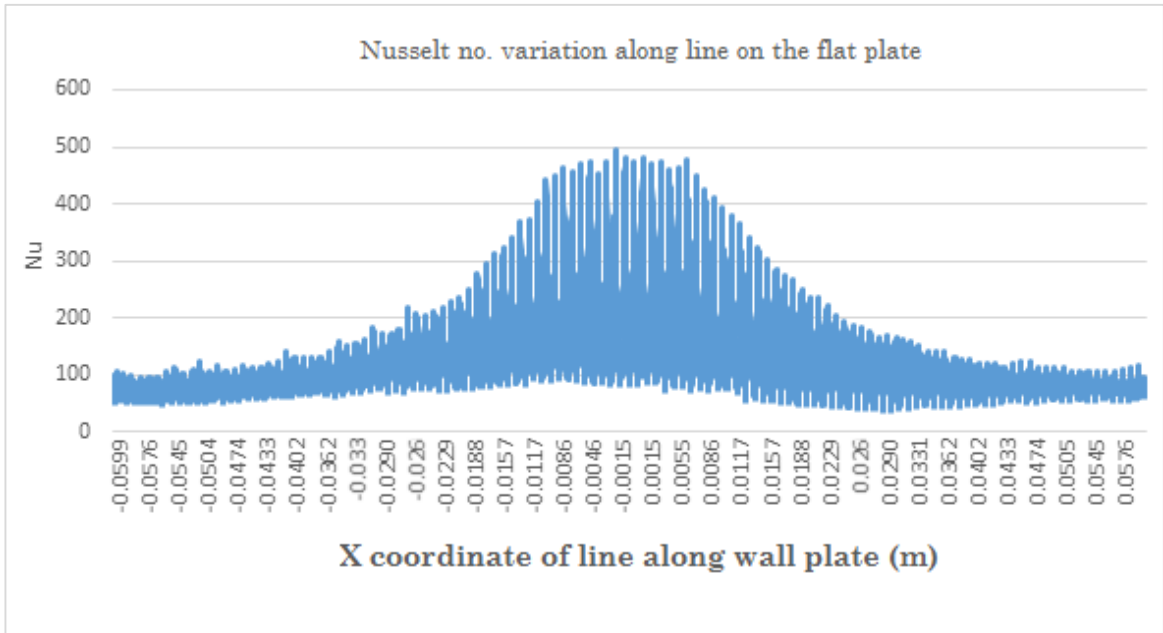


Figure 13 Dimensionless plot of Nu vs X in this study at $n=0.8$ and velocity= 1.5 m/s.

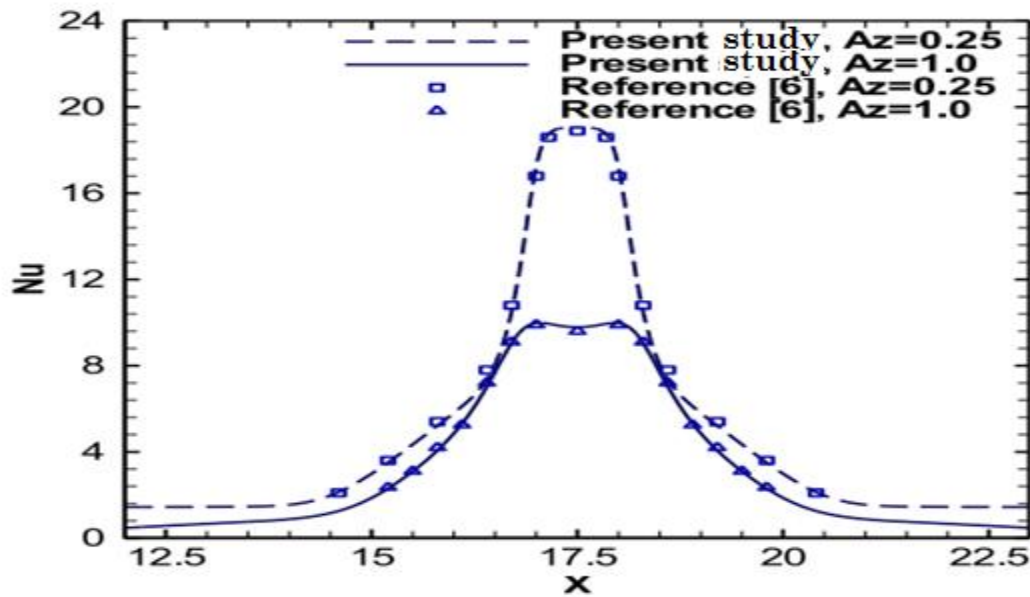


Figure 14 Variation of Nu vs X present in literature [15]

Results and Discussion

This chapter deals with the detailed 3D simulation results obtained for the previously defined flow of the jet. The specifications of the non-Newtonian fluid used are tabulated in the table 3.4 (a) whereas the properties of the flat plate material used are tabulated in table 3.4 (b). The result section has been divided in two parts according to the two different velocities used, which are 0.5 m/s as well as 1.5 m/s. Up again until process attained a dynamic steady state, the unsteady calculations were performed. The time step size used is 0.01.

The first section of result compares the contours, streamlines and other parameters for inlet velocity of $v=0.5$ m/s.

The outline of results obtained are as :

- The velocity contours, velocity streamline, velocity vectors are shown for different power law fluids on an introduced y-z plane in the model.
- The Temperature contour and Nusselt number contour on the flat plate have been shown.
- A radial line with 50 intermediate points is introduced along the heated wall plate at the centreline. Along this line, the temperature variation, Nusselt number variation has been shown.

Case 1: When inlet velocity has been considered as 0.5 m/s and power law is varied.

4.1 Inlet jet Velocity

The time averaged contours of impingement inlet velocity are obtained and are shown for increasing power-law index values from 0.6 to 1.6, for the inlet velocity of $v = 0.5$ m/s (Fig. 15-20) . The velocity streamlines are shown in Fig.21-26 , and the corresponding velocity vectors are shown in Fig.27-32.

The estimated heat transfer rates on the plates are significantly impacted by the jet's velocity. Increasing the jet velocity provides an enhanced cooling capacity of the jet. From literature

if can be seen that the heat transfer rate depends on the Reynolds number, and the Re no. depends on the velocity, resulting in a better cooling effect for higher velocity jets.

The core is vital for heat transfer, throughout addition to the jet's speed. It specifies the numerous flow zones and the thickness of the jet in a radial direction after the collision, as well as the severity of the jet's effect on the surface. As shown in the figures of velocity contours and the streamlines of Pseudoplastic fluids, it shows the flow development in radial direction and its thickness decreases as moving away from the center of impingement. This implies that the increment in stress due to flow, the fluid thins out rapidly in the radial direction. This happens because the jet's outer layer is pulled apart by drag forces, which rips the jet and causes it to continue spreading.

Since the shear-thinning fluids' fluidity rises as stress rises, they stick to surfaces more quickly, which improves the cooling effect. The impinged jet's centre, which is fuller and thicker, reaches the target wall surface. The flow of the jet will divert depending on how much pressure it loses before hitting the surface, according to the continuity equation. As we know from the literature [15], the smaller is the distance of impingement, the larger does the jet spreads. Thereby vortices in velocity streamlines gets away from the impinged center. Hence, while comparing the streamlines for different power-law fluids, the vortices formed shows the greater flow thinning for Pseudoplastic fluids and better flow development after impinging the target surface.

Whereas for the shear-thickening fluids (Dilatant fluids), shows a narrow jet core and the length is also short. This is evident because the shear stress, which is indicated on the jet's outer portion, causes the fluid to act as a semi-solid object that is attempting to flow. As a result, there is no proper continuous contact with the plate and a reduction in the ability to cool with dilatant fluids is seen. As can be observed from the jet's input velocity of 1.5 m/s, the length of the core is proportional to that speed. Higher velocities exhibit better cooling characteristics, as evidenced by temperature change.

For a constant velocity, higher Nusselt number and lower Temperature is obtained for Pseudoplastic fluid, which implies better cooling characteristics. The Dilatant fluids shows poor cooling characteristics while Newtonian fluids shows better performance than dilatant fluids.

1.Velocity contours obtained for varying power-law index n, at velocity=0.5 m/s :

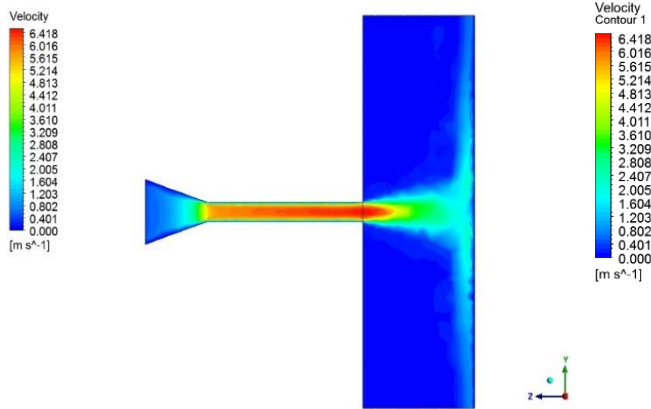


Figure 15 velocity contour at n=0.6 and velocity=0.5m/s

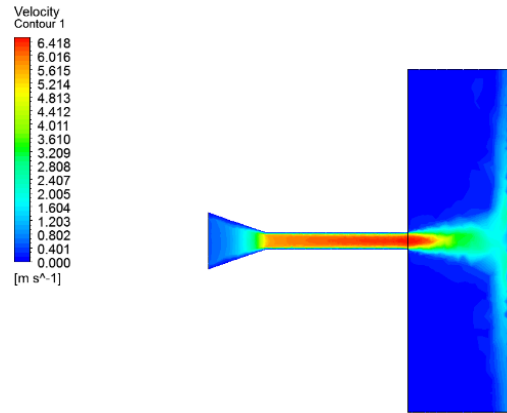


Figure 16 velocity contour at n=0.8 and velocity=0.5m/s

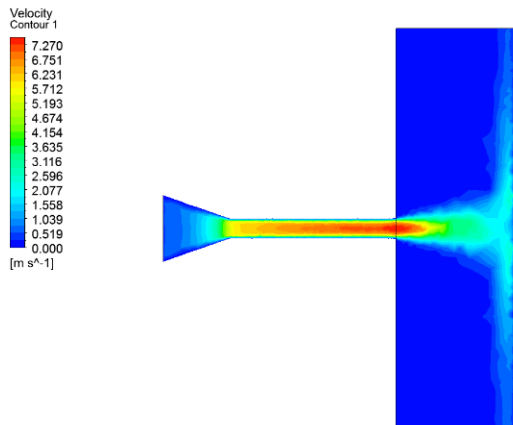


Figure 17 velocity contour at n=1.0 and velocity=0.5m/s.

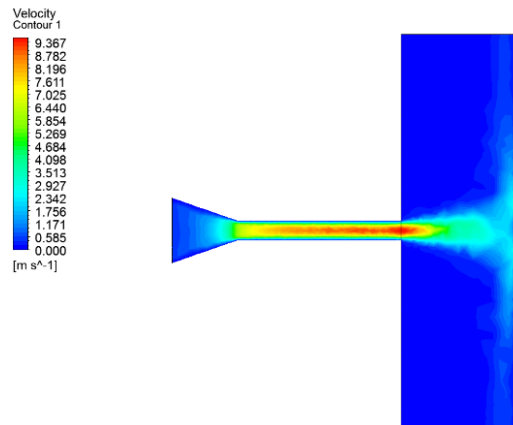


Figure 18 velocity contour at n=1.2 and velocity=0.5m/s.

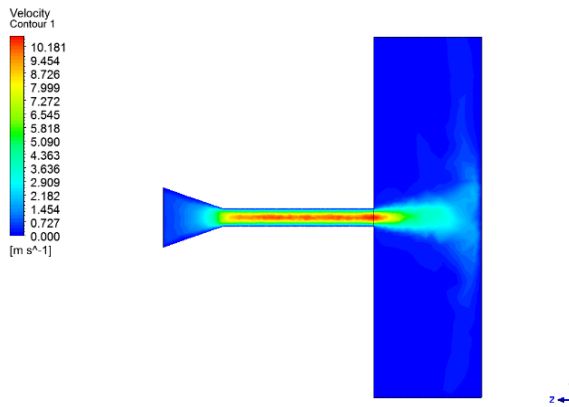


Figure 19 velocity contour at n=1.4, and velocity=0.5m/s.

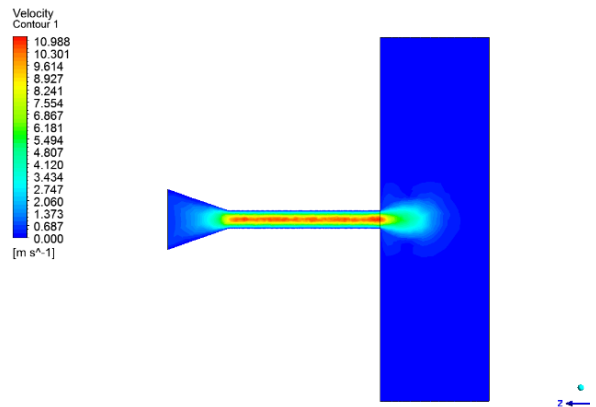


Figure 20 velocity contour at n=1.6 and velocity=0.5m/s.

2. Velocity streamlines obtained for varying power-law index n , at velocity=0.5 m/s :

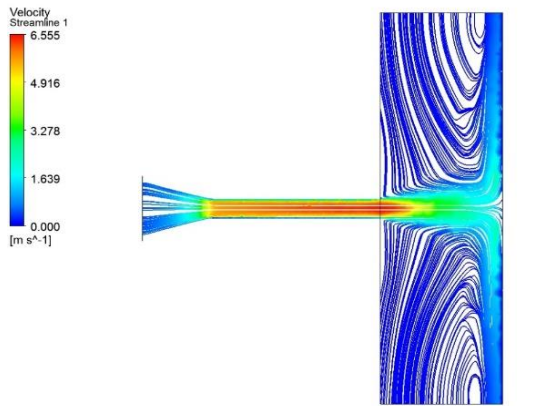


Figure 21 velocity streamline at $n=0.6$ and velocity=0.5m/s.

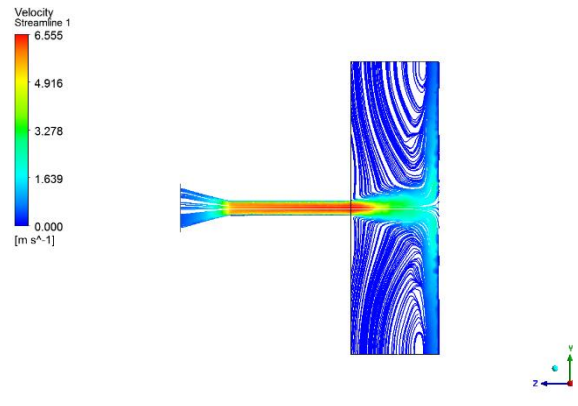


Figure 22 velocity streamline at $n=0.8$ and velocity=0.5m/s.

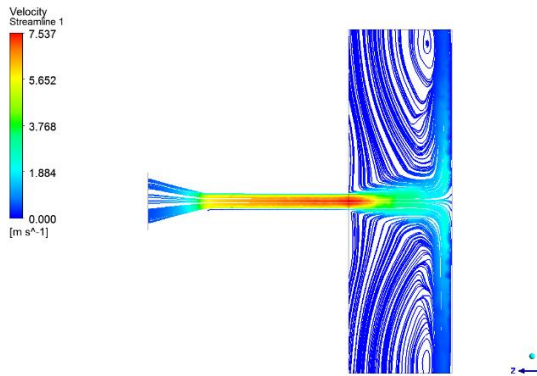


Figure 23 velocity streamline at $n=1.0$ and velocity=0.5m/s.

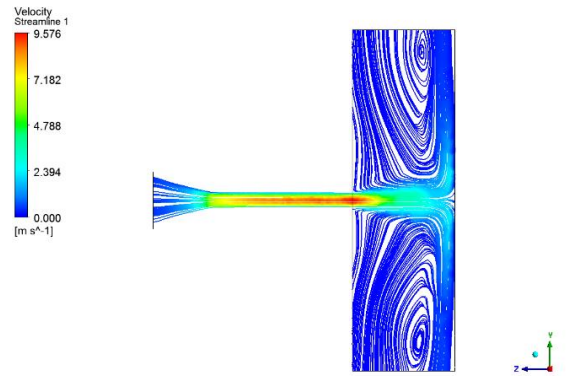


Figure 24 velocity streamline at $n=1.2$ and velocity=0.5m/s.

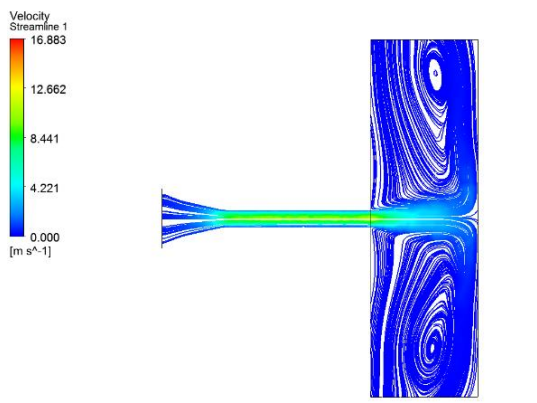


Figure 25 velocity streamline at $n=1.4$ and velocity=0.5m/s.

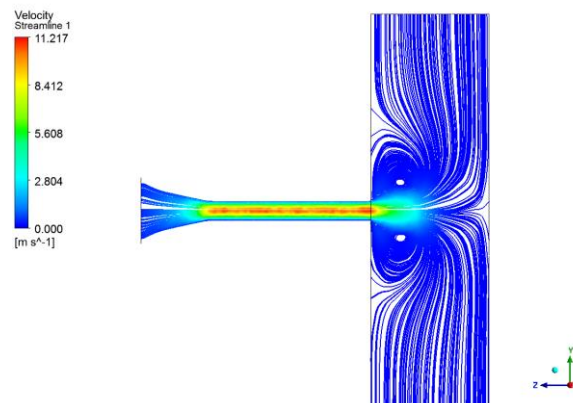


Figure 26 velocity streamline at $n=1.6$ and velocity=0.5m/s.

3. Velocity vector obtained for varying power-law index n at velocity=0.5 m/s :

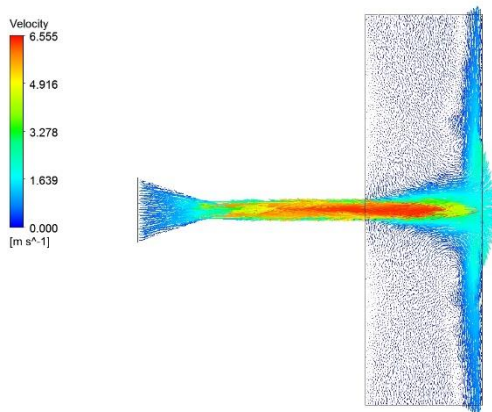


Figure 27 velocity vector at $n=0.6$ and velocity=0.5m/s.

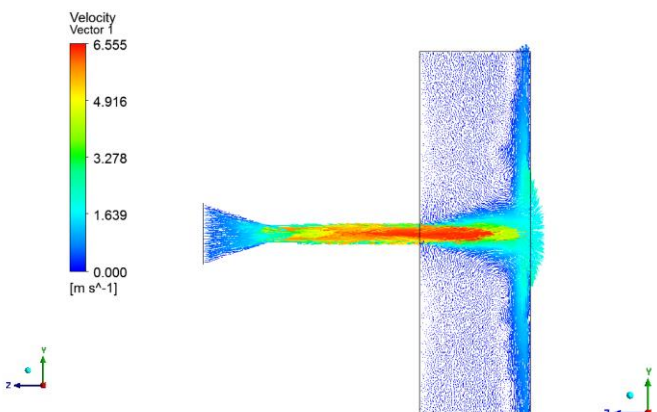


Figure 28 velocity vector at $n=0.8$ and velocity=0.5m/s.

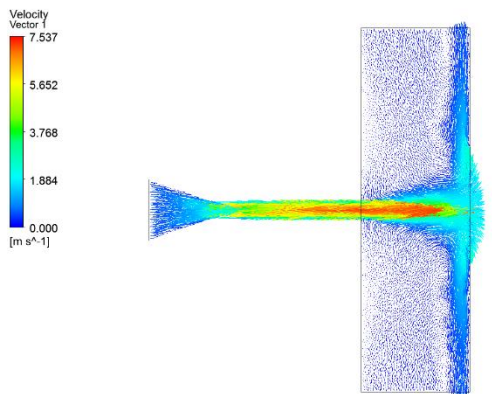


Figure 29 velocity vector at $n=1.0$ and velocity=0.5m/s.

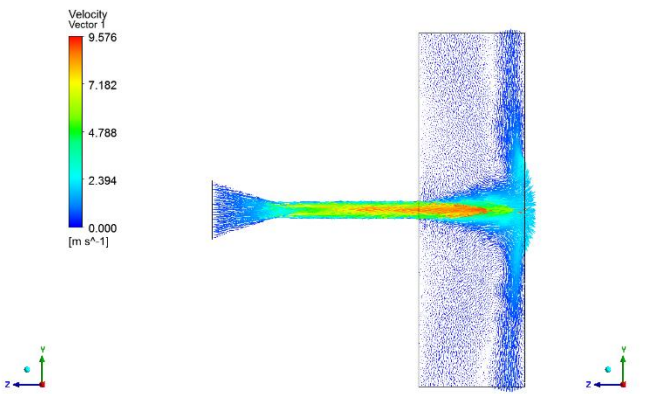


Figure 30 velocity vector at $n=1.2$ and velocity=0.5m/s.

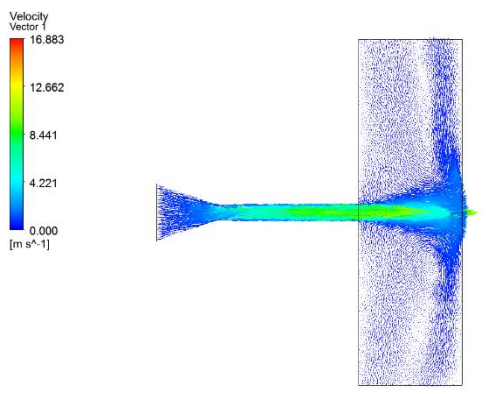


Figure 31 velocity vector at $n=1.4$ and velocity=0.5m/s.

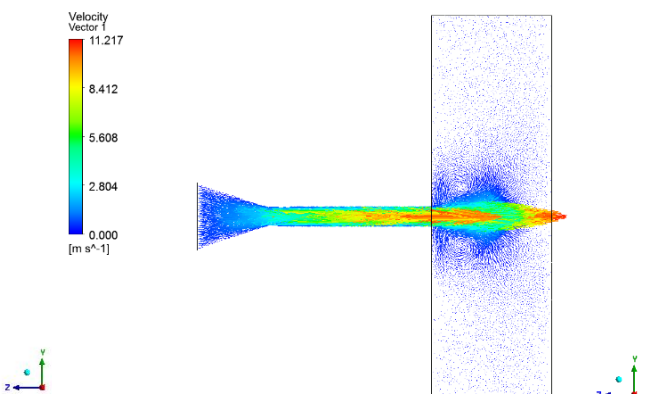


Figure 32 velocity vector at $n=1.6$ and velocity=0.5m/s.

4. Temperature contours obtained for varying power-law index n, at velocity=0.5 m/s :

The temperature contours shows the variation of temperature in radial direction after the impingement. It is observed that larger zones of low temperature values are present on the plate for lower power-law index, which gets smaller as we increase the value of the index. This shows better cooling characteristics of pseudoplastic fluid jets than corresponding higher powerlaw index fluids.

Similarly for Nusselt number contours a clear visible zone of higher nusselt number centralized towards the core of the impinged area can be seen, which gets smaller and unevenly distributed as we increase the power-law index.

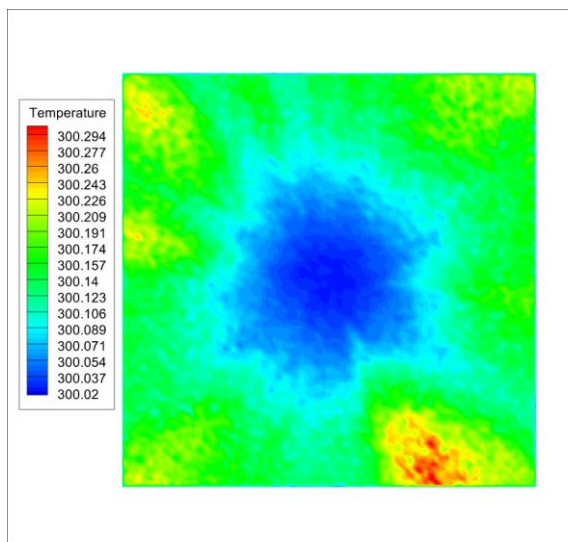


Figure 33 Temperature contour at n=0.6 and velocity=0.5m/s.

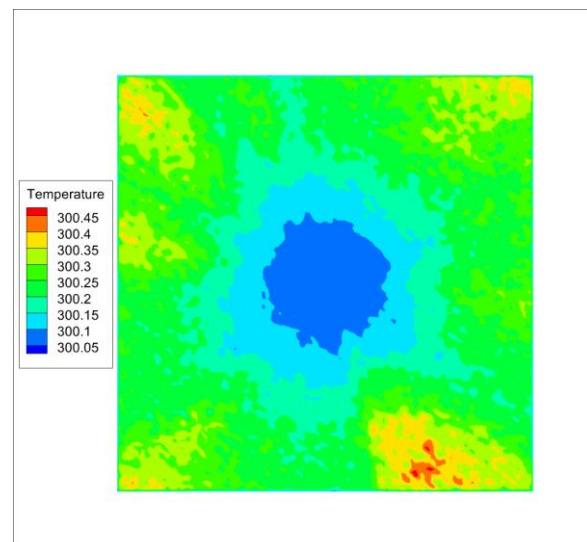


Figure 34 Temperature contour at n=0.8 and velocity=0.5m/s.

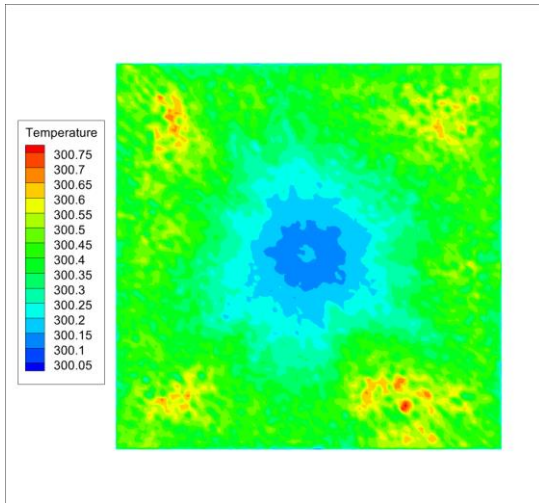


Figure 35 Temperature contour at $n=1.0$ and velocity $=0.5\text{m/s}$.

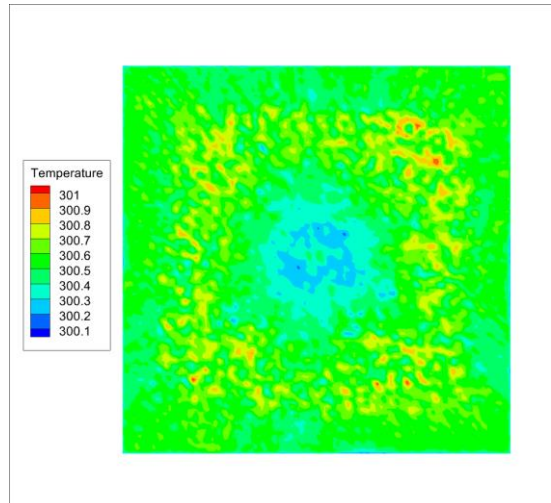


Figure 36 temperature contour at $n=1.2$ and velocity $=0.5\text{m/s}$.

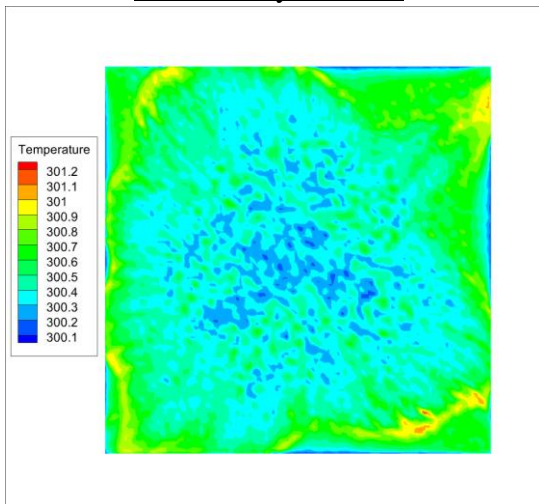


Figure 37 temperature contour at $n=1.4$ and velocity $v=0.5\text{m/s}$.

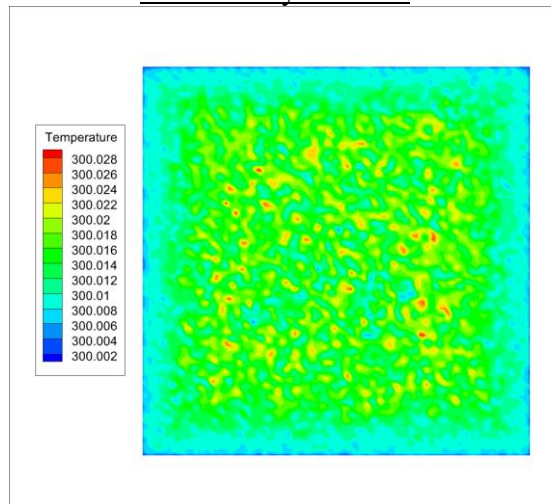


Figure 38 temperature contour at $n=1.6$ and velocity $v=0.5\text{m/s}$.

5. Nusselt no. contour obtained for varying power-law index n , at velocity = 0.5 m/s :

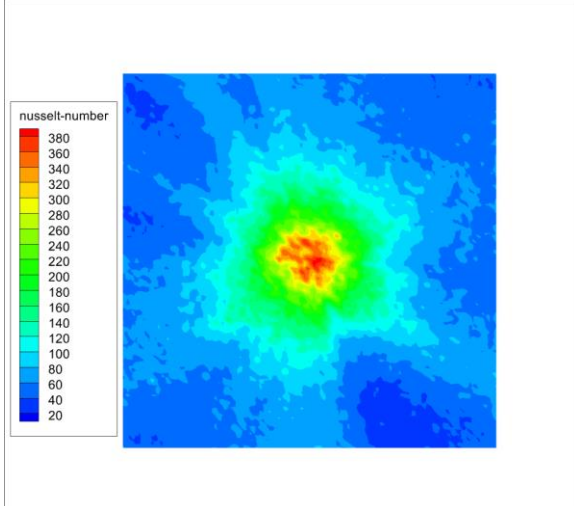


Figure 39 Nusselt no. contour at $n=0.6$ and velocity = 0.5m/s.

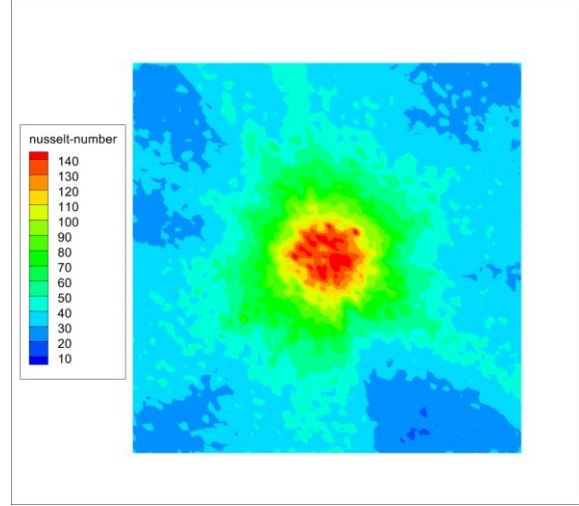


Figure 40 Nusselt no. contour at $n=0.8$ and velocity = 0.5m/s.

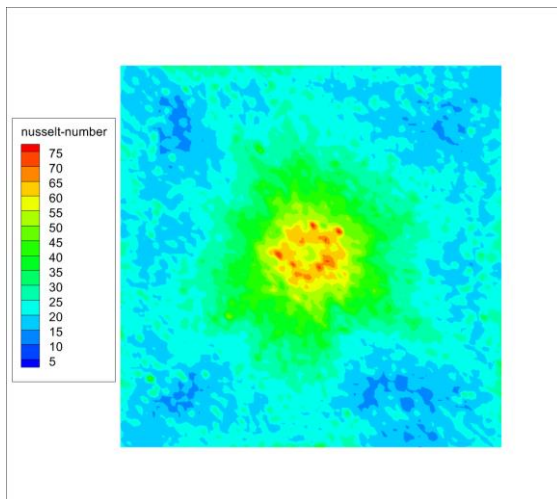


Figure 41 Nusselt no. contour at $n=1.0$ and velocity = 0.5m/s

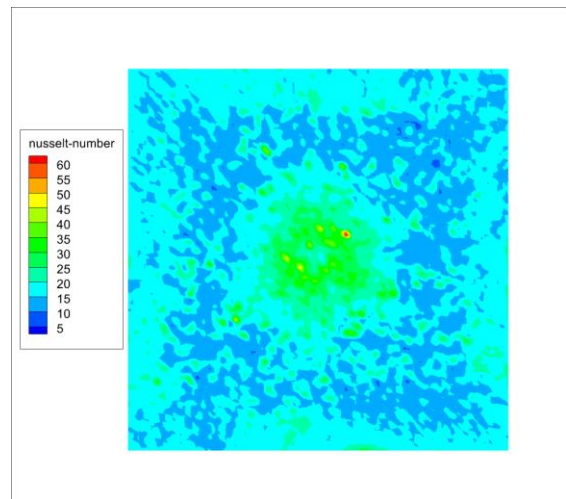


Figure 42 Nusselt no. contour at $n=1.2$ and velocity = 0.5m/s

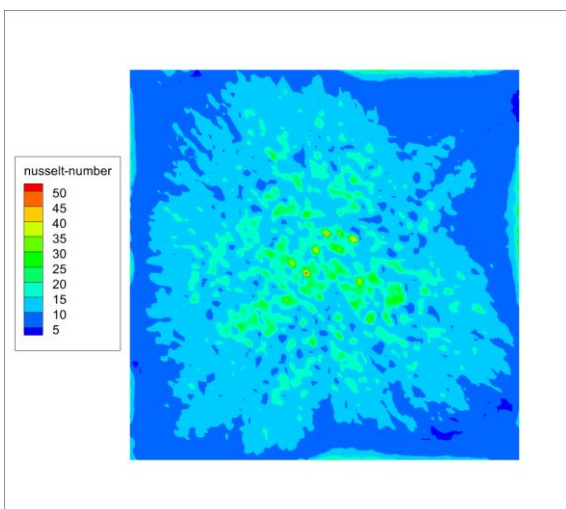


Figure 43 Nusselt no. contour at $n=1.4$ and velocity = 0.5m/s

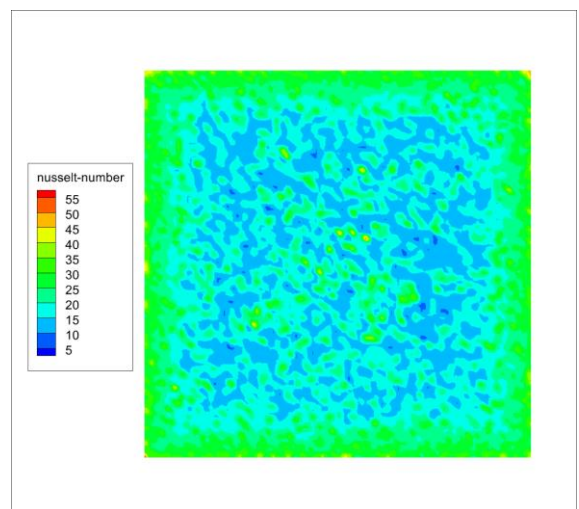


Figure 44 Nusselt no. contour at $n=1.6$ and velocity = 0.5m/s

6. Temperature vs x coordinate variation chart plotted at the line drawn along the heated wall plate , for varying n at v= 0.5m/s :

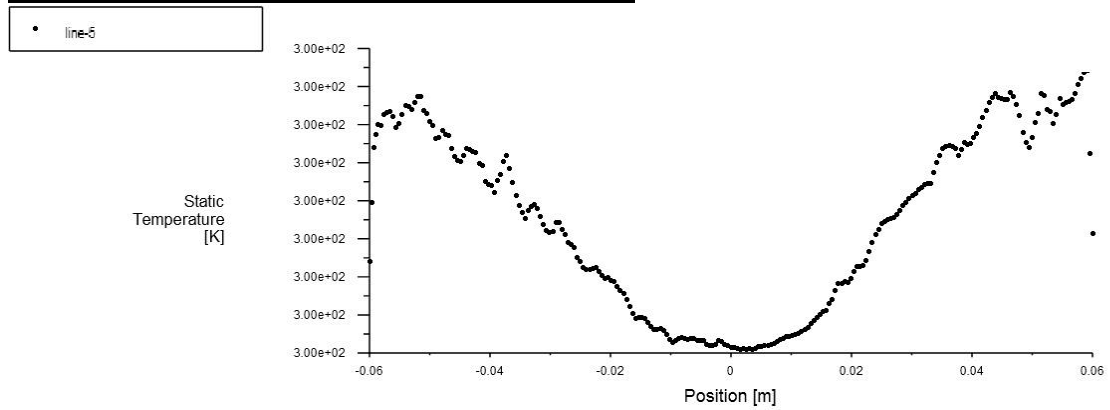


Figure 45 Temperature variation along line, at n=0.6 and velocity=0.5m/s.

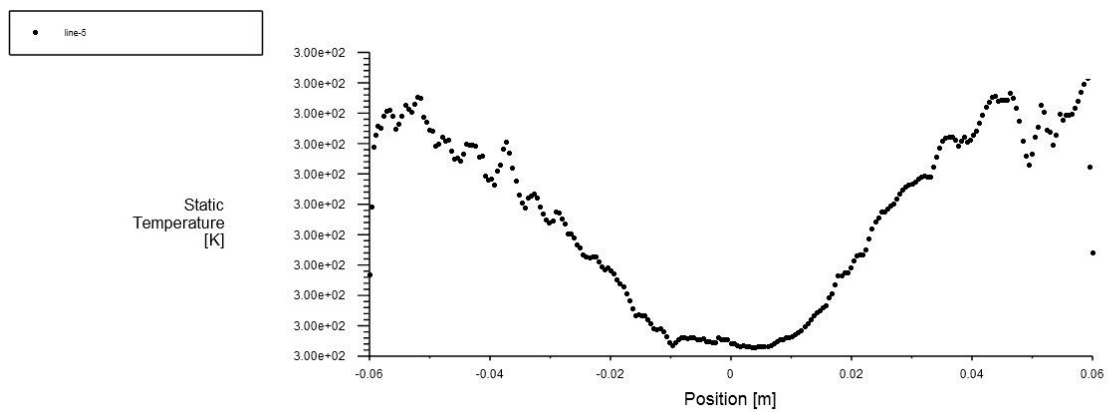


Figure 46 Temperature variation along line, at n=0.8 and velocity=0.5m/s.

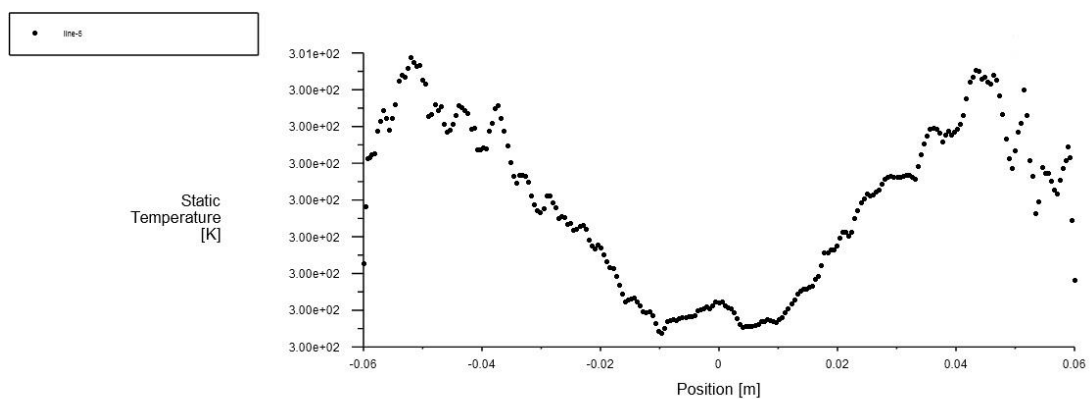


Figure 47 Temperature variation along line, at n=1.0 and velocity=0.5m/s.

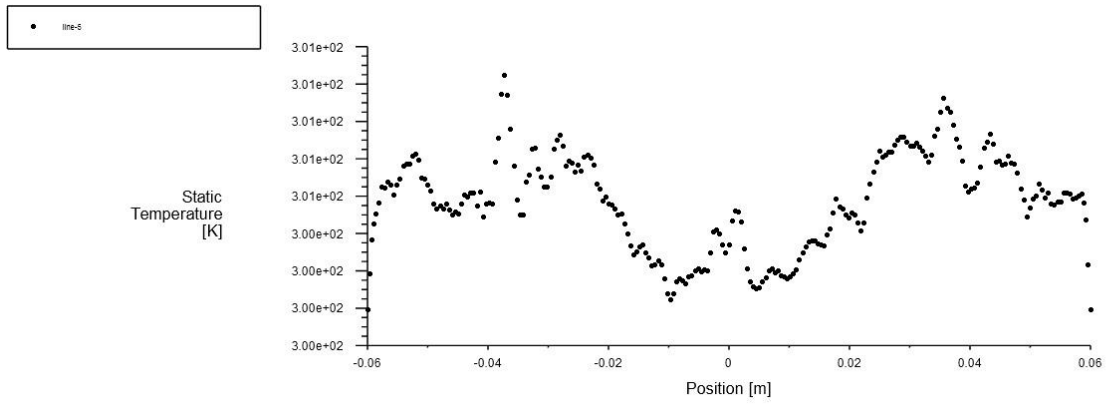


Figure 48 Temperature variation along line, at n=1.2 and velocity=0.5m/s.

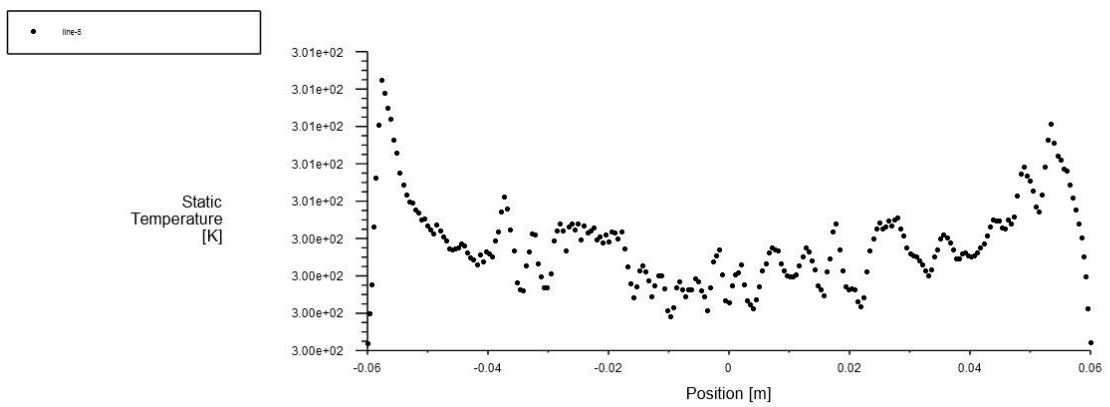


Figure 49 Temperature variation along line, at n=1.4 and velocity=0.5m/s.

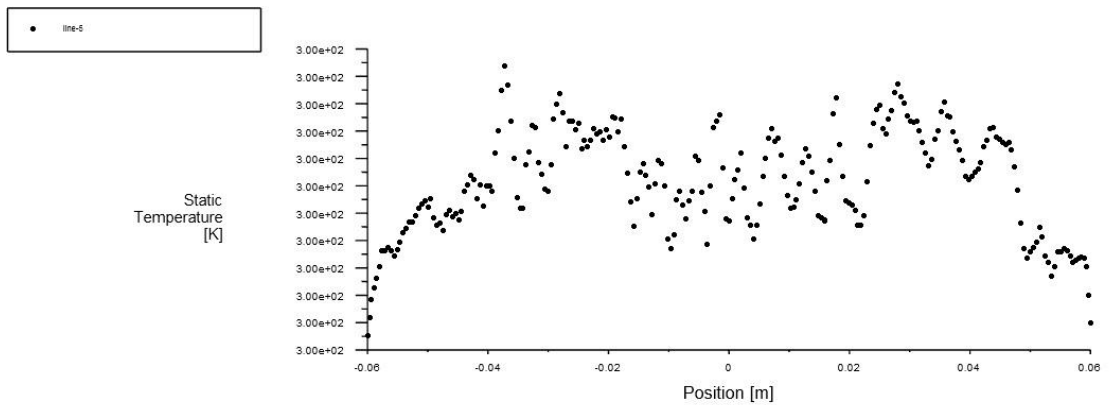


Figure 50 Temperature variation along line, at n=1.6 and velocity=0.5m/s.

7. Nusselt no. vs x coordinate variation chart plotted at the line drawn along the heated wall plate , for varying n, v= 0.5m/s :

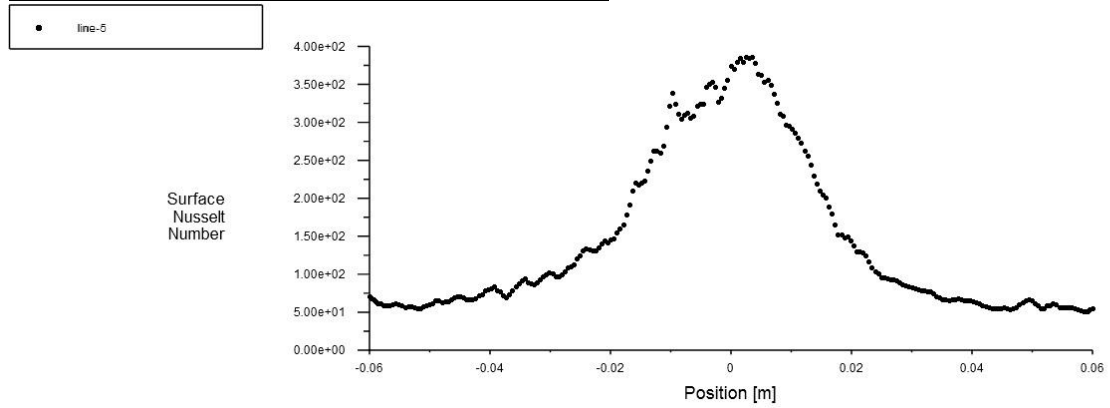


Figure 51 Nusselt no. variation along line, at n=0.6 and velocity=0.5m/s.

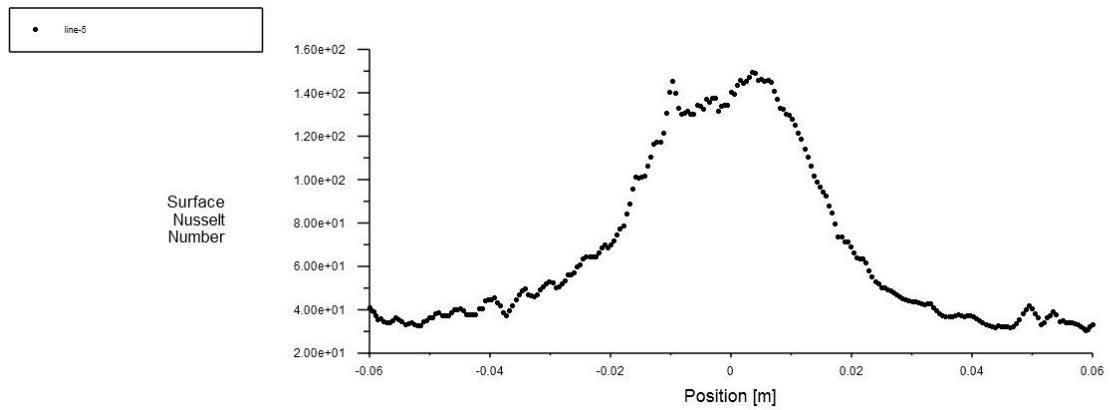


Figure 52 Nusselt no. variation along line, at n=0.8 and velocity=0.5m/s.

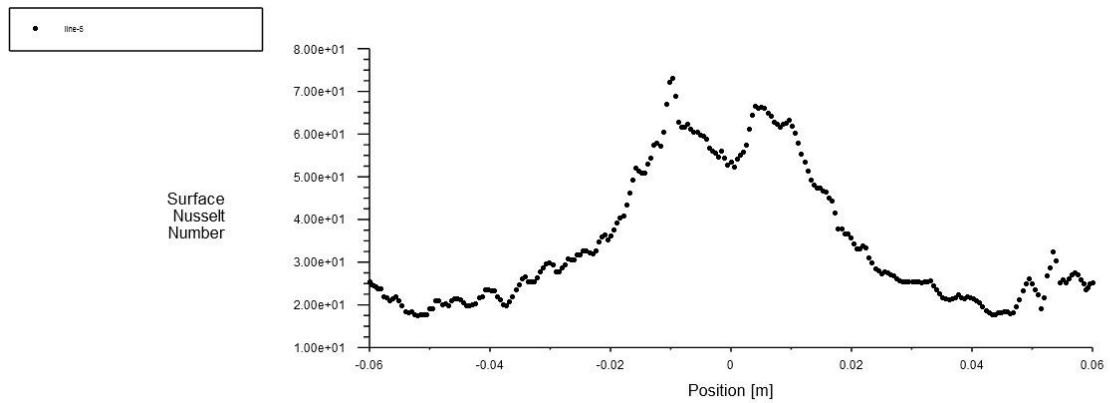


Figure 53 Nusselt no. variation along line, at n=1.0 and velocity=0.5m/s.

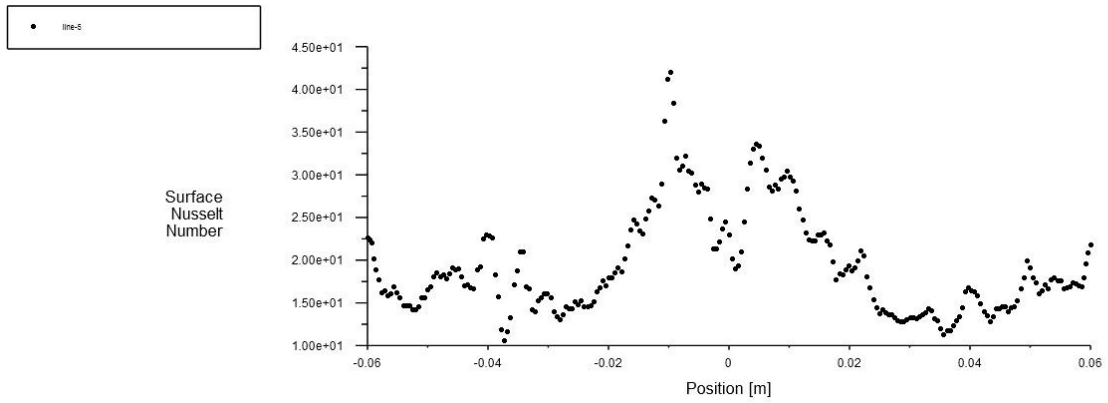


Figure 54 Nusselt no. variation along line, at n=1.2 and velocity=0.5m/s.

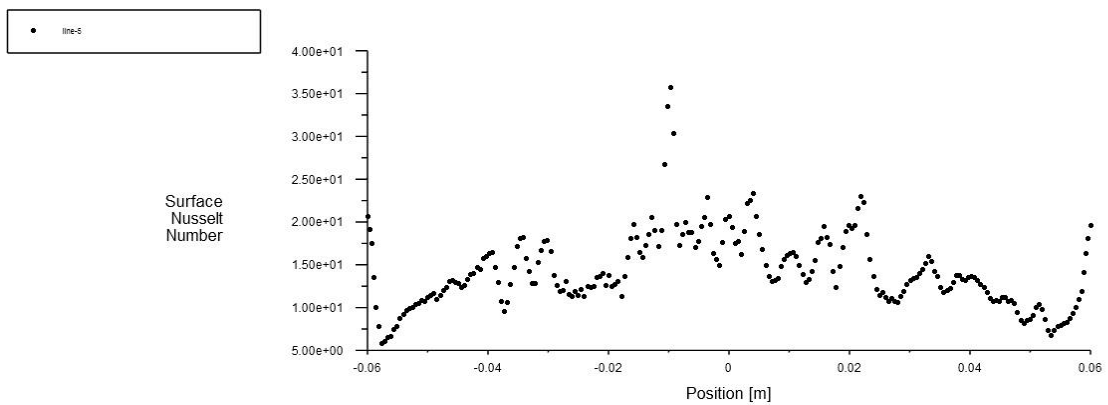


Figure 55 Nusselt no. variation along line, at n=1.4 and velocity=0.5m/s.

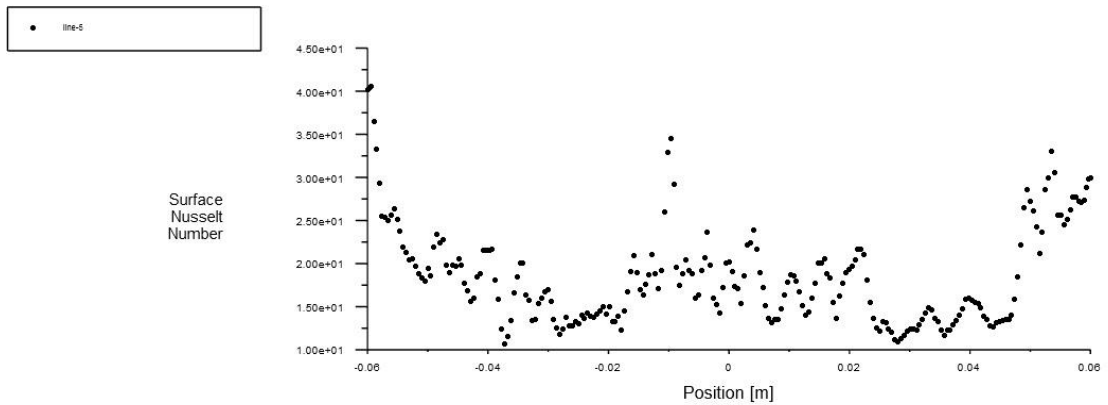


Figure 56 Nusselt no. variation along line, at n=1.6 and velocity=0.5m/s.

The above section shown the various observed results for velocity of 0.5 m/s, whereas in this section, velocity has been increased to 1.5 m/s, to study the same parameters and a comparison has been made.

The Nusselt number observations:

The variation of Nusselt number with increasing power law index is shown in the figure 58, where it shows that with increase in power law index, the Nu value decreases, whereas for higher velocities we have higher Nusselt number obtained. This implies that for a higher velocity better heat transfer characteristics is observed, and also for shear thickening fluids, poorer characters were shown.

The Nusselt number vs dimensionless lateral length (x/W) along a line on the flat plate is shown in the Figure 57 , velocity at inlet of 1.5 m/s. A sudden increment in Nu distribution is observed, this happens as a result of the impinged jet's abrupt splashing action after striking the surface.

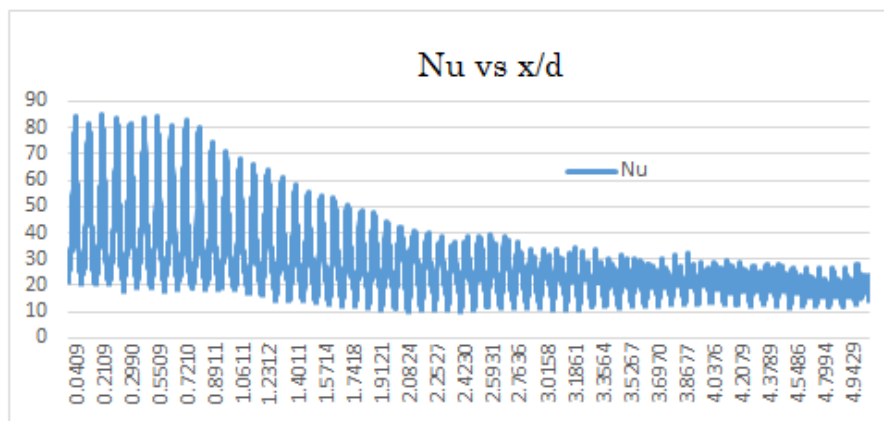


Figure 57 Nusselt number variation with dimensionless position when $v = 1.5$ m/s

The Pseudoplastic fluids shows a higher jet velocity and circulation effects in the boundary layer, which readily impacts the heat transfer characteristics. Additionally, the heat transmission with the plate is impacted by the radial velocity.

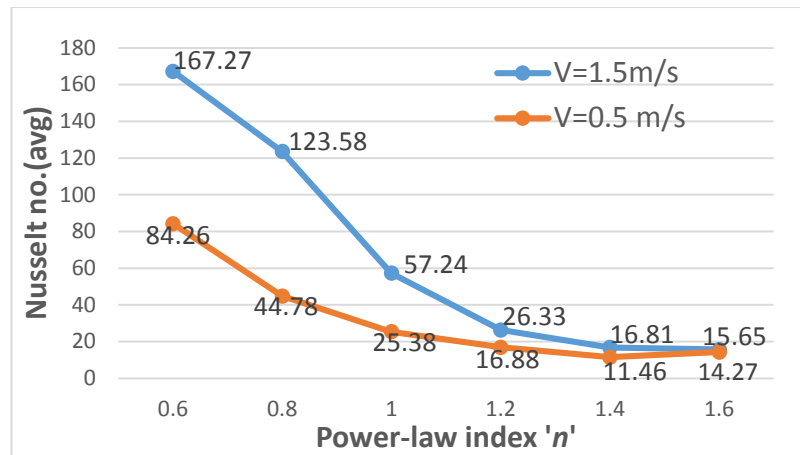


Figure 58 Variation of Nu for V=1.5 m/s in the dimensionless lateral position.

For the Dilatant fluids shorter cores are observed, hence the fluids doesn't spread radially over the surface of the flat plate. Instead, it bounces off the surface like a semi solid. This provides a poor heat transfer property. This mainly occurred for $n=1.4$ and 1.6 . As increasing the power-law index enhances the semi solid properties of the fluid. Poor cooling can be expected, still there is a few amounts of heat transfer occurred on the flat surface. It is also observed from the temperature variation along the line drawn on the plate.

A sense of the severity of the fluid impingement, the impingement velocity, and the phenomena at the plate can be gained from the length of the core. When shear thickening or dilatant fluids are used, the length of the core is observed to be substantially shorter than when shear thinning fluids are used. As we raise the fluid's velocity, the core's length does, however, grow longer.

Hence the simulation results obtained after applying velocity at inlet of 1.5 m/s is shown in the subsequent section.

6. Results obtained for varying n and inlet velocity $v=1.5$ m/s :

6.1.Velocity contours obtained for varying power-law index n, at velocity=1.5 m/s :

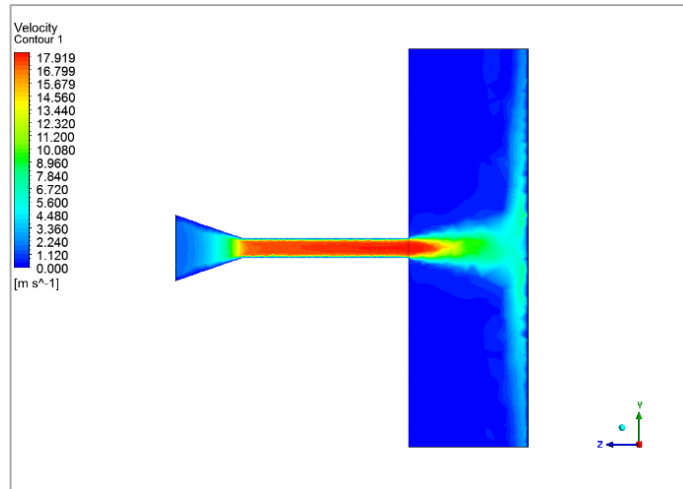


Figure 59 velocity contour at $n=0.6$ and velocity=1.5m/s

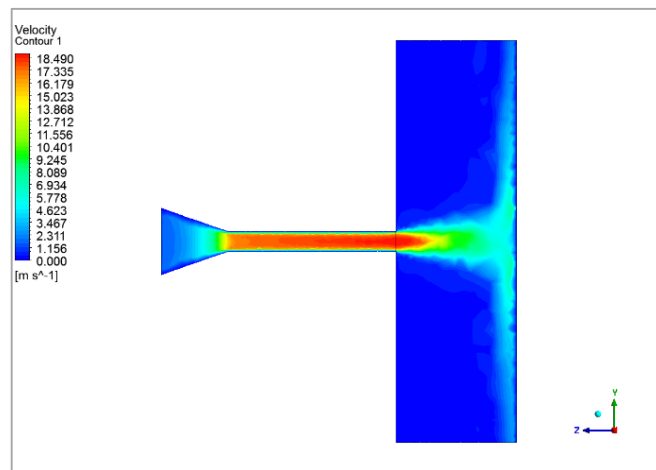


Figure 60 velocity contour at $n=0.8$ and velocity=1.5m/s

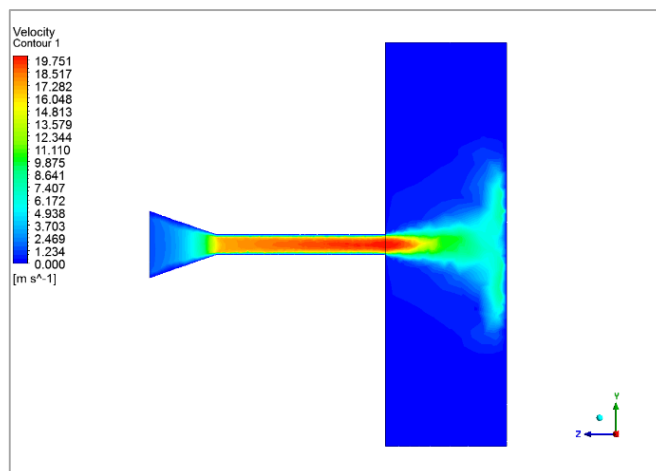


Figure 61 velocity contour at $n=1.0$ and velocity=1.5m/s

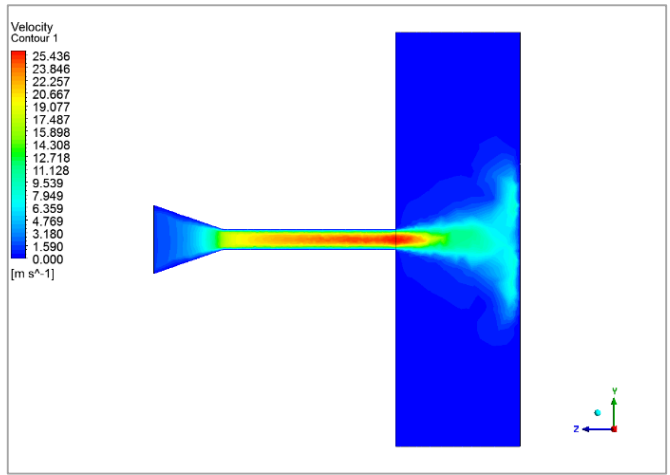


Figure 62 velocity contour at $n=1.2$ and velocity=1.5m/s

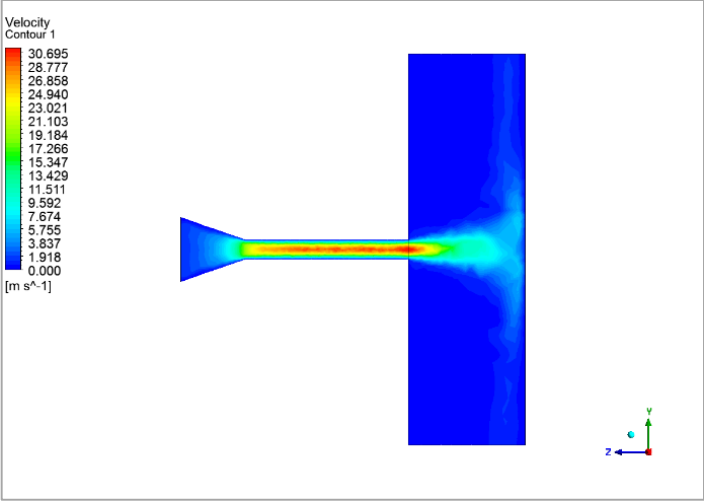


Figure 63 velocity contour at $n=1.4$ and velocity=1.5m/s

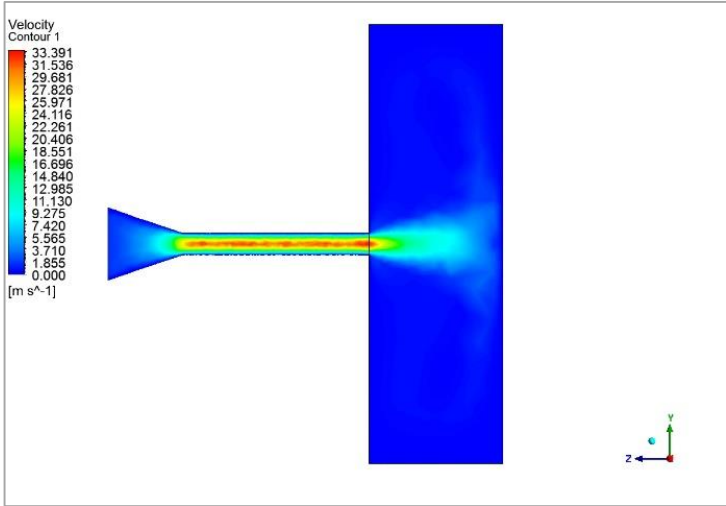


Figure 64 velocity contour at $n=1.6$ and velocity=1.5m/s

6.2 Velocity streamlines obtained for varying power-law index n , velocity=1.5 m/s :

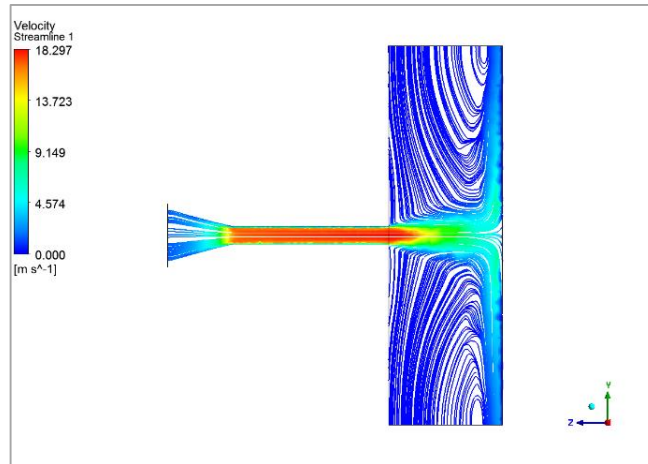


Figure 65 velocity streamline at $n=0.6$ and velocity=1.5m/s

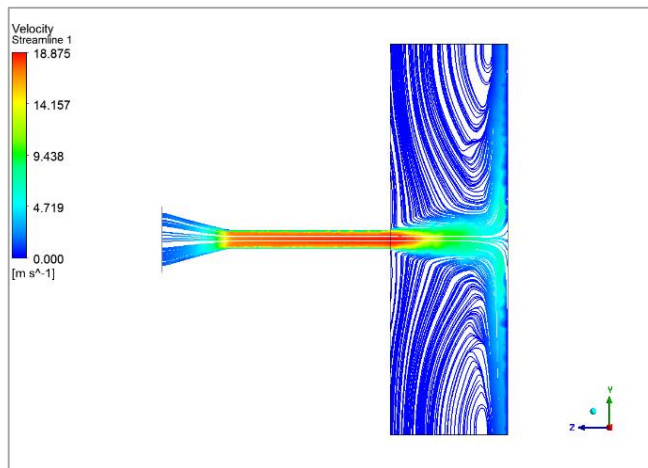


Figure 66 velocity streamline at $n=0.8$ and velocity=1.5m/s

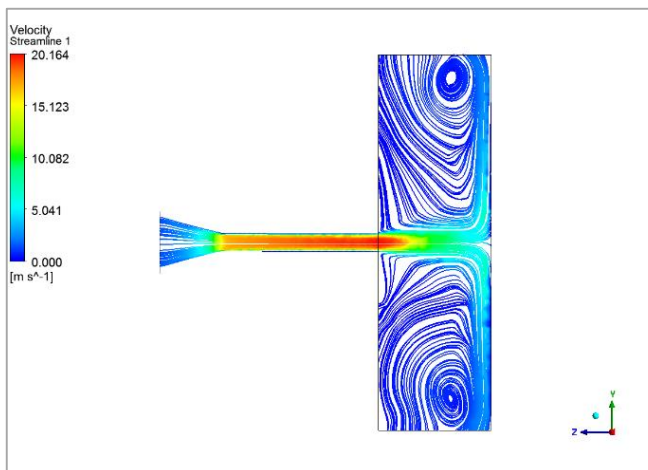


Figure 67 velocity streamline at $n=1.0$ and velocity=1.5m/s

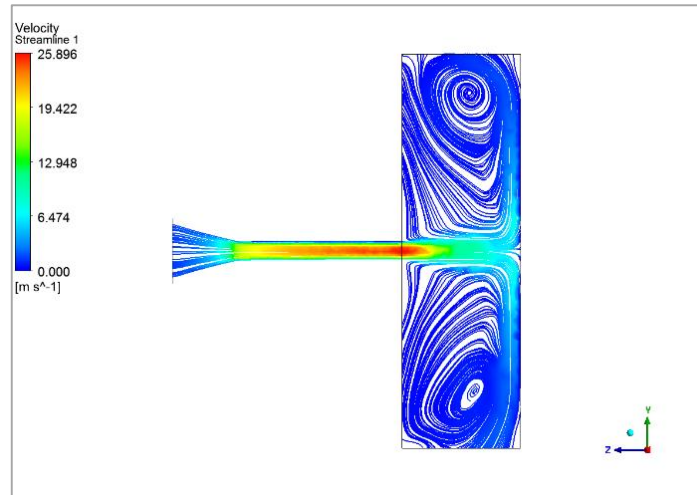


Figure 68 velocity streamline at $n=1.2$ and velocity= 1.5m/s

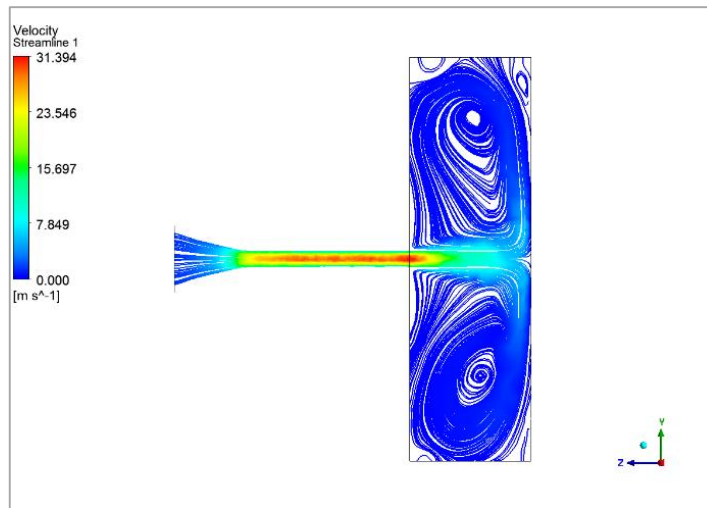


Figure 69 velocity streamline at $n=1.4$ and velocity= 1.5m/s

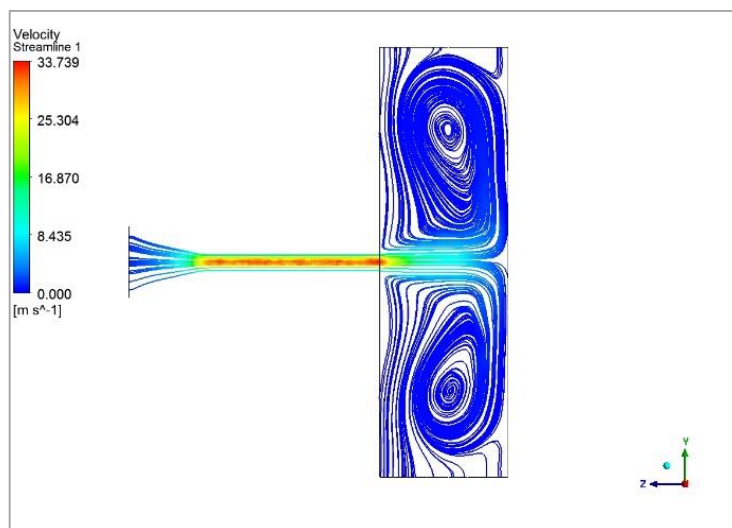


Figure 70 velocity streamline at $n=1.6$ and velocity= 1.5m/s

6.3 Velocity vector obtained for varying power-law index n , at velocity=1.5 m/s :

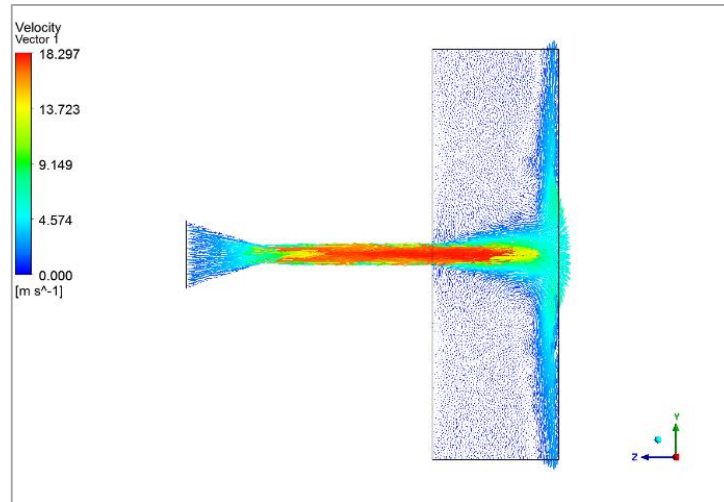


Figure 71 velocity vector at $n=0.6$ and velocity=1.5m/s

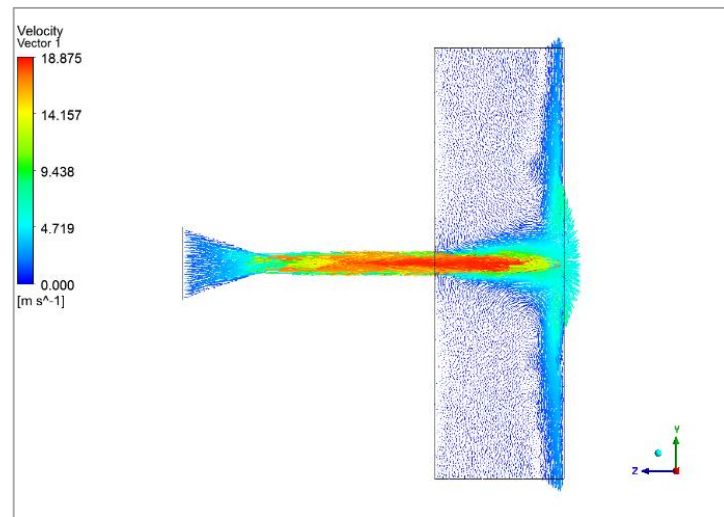


Figure 72 velocity vector at $n=0.8$ and velocity=1.5m/s

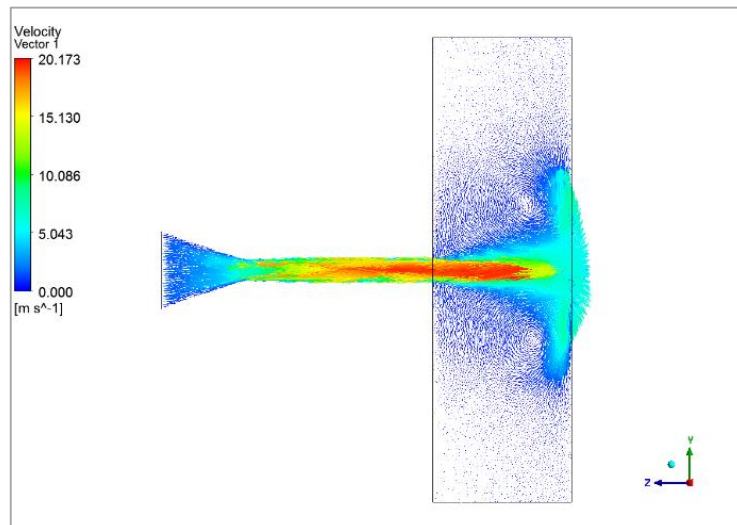


Figure 73 velocity vector at $n=1.0$ and velocity=1.5m/s

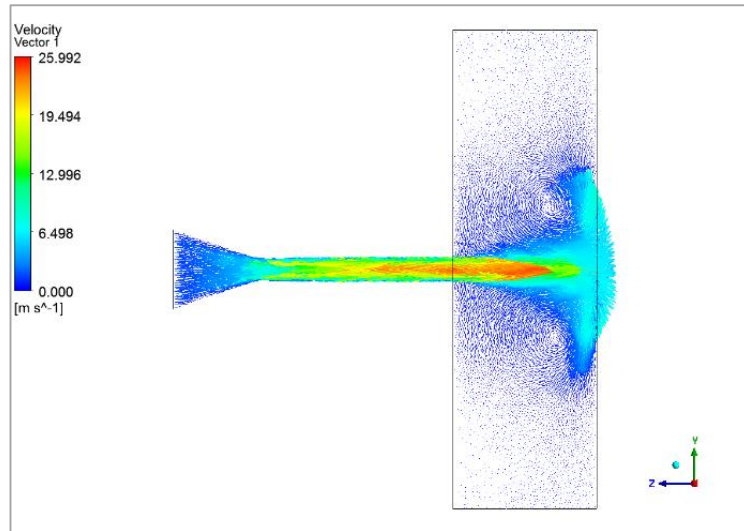


Figure 74 velocity vector at n=1.2 and velocity=1.5m/s

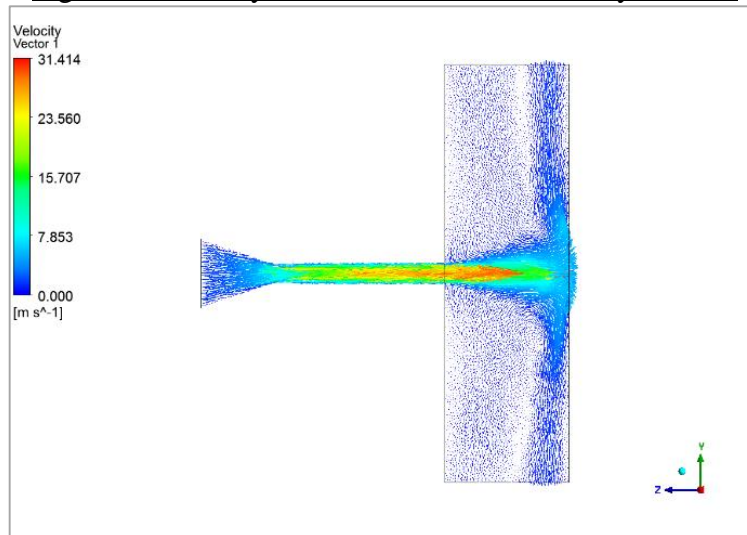


Figure 75 velocity vector at n=1.4 and velocity=1.5m/s

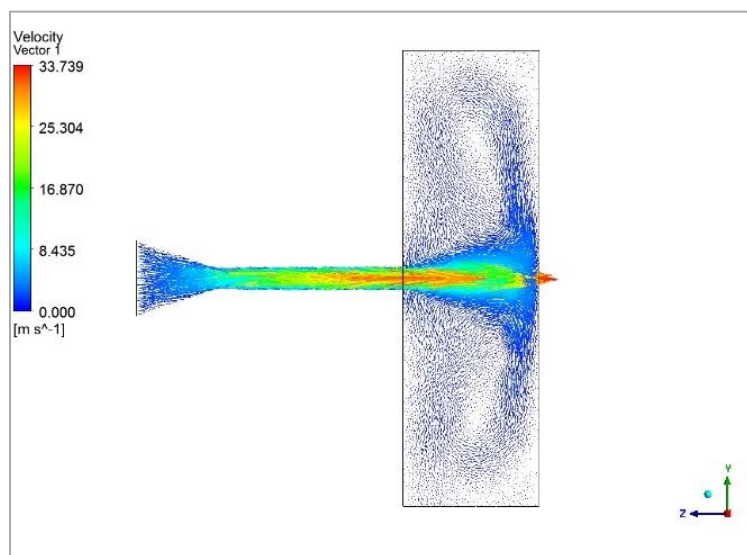


Figure 76 velocity vector at n=1.6 and velocity=1.5m/s

6.4 Temperature contour obtained for varving power-law index n, at velocity=1.5 m/s :

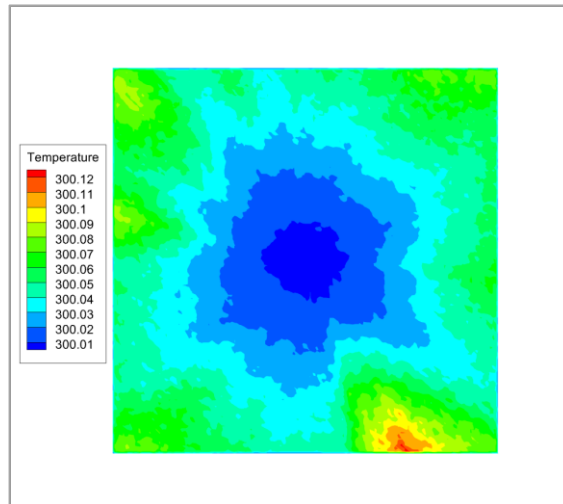


Figure 77 Temperature contour at n=0.6 and velocity=1.5m/s

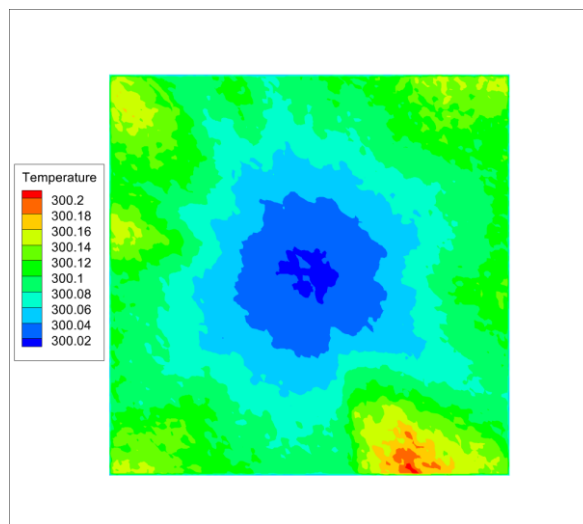


Figure 78 Temperature contour at n=0.8 and velocity=1.5m/s

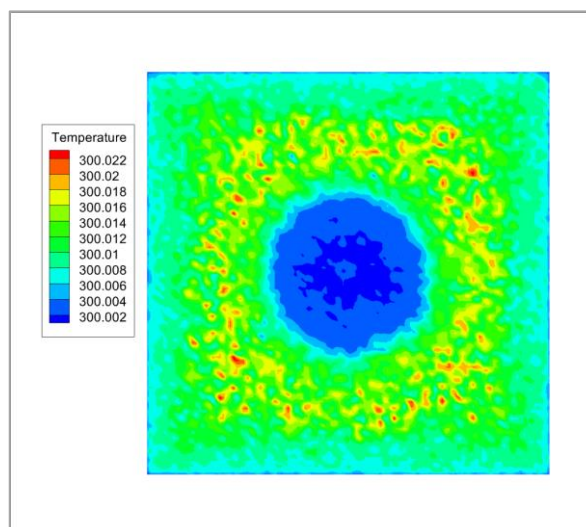


Figure 79 Temperature contour at n=1.0 and velocity=1.5m/s

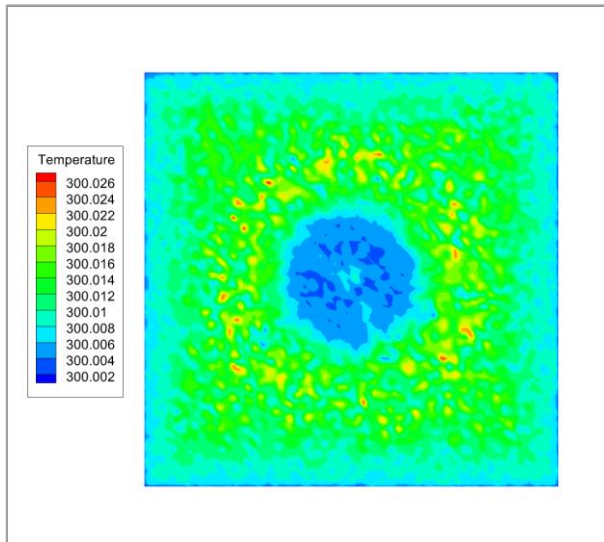


Figure 80 Temperature contour at $n=1.2$ and velocity=1.5m/s

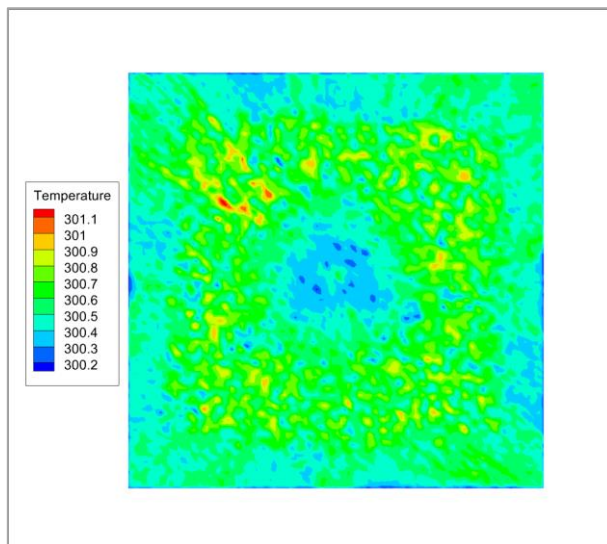


Figure 81 Temperature contour at $n=1.4$ and velocity=1.5m/s

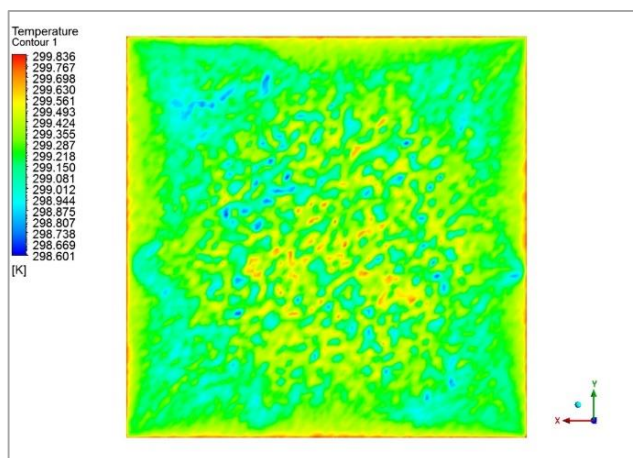


Figure 82 Temperature contour at $n=1.6$ and velocity=1.5m/s

6.5 Nusselt no. contour obtained for varying power-law index n , at velocity=1.5 m/s :

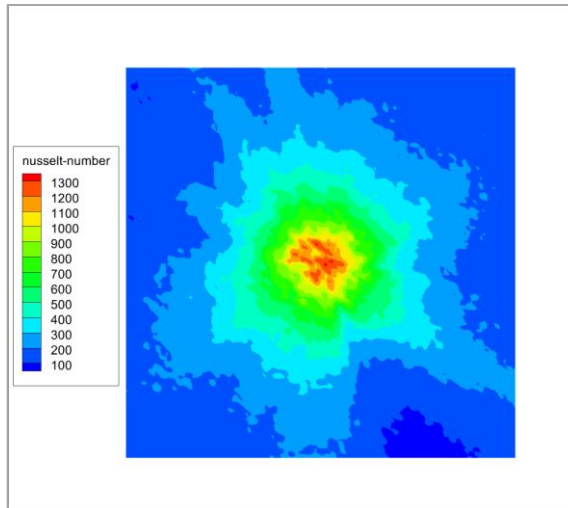


Figure 83 Nusselt no. at $n=0.6$ and velocity=1.5m/s

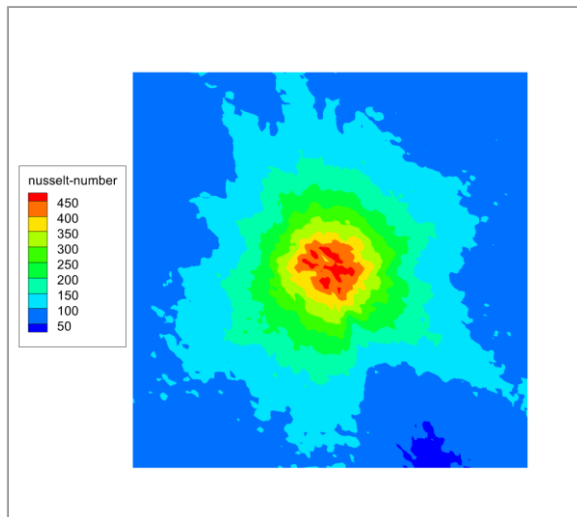


Figure 84 Nusselt no. at $n=0.8$ and velocity=1.5m/s

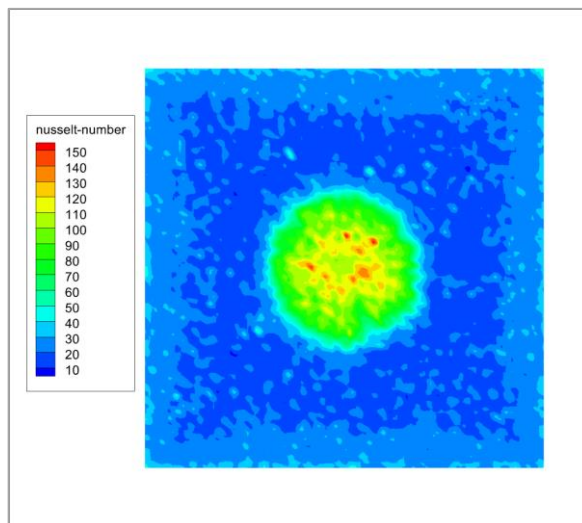


Figure 85 Nusselt no. at $n=1.0$ and velocity=1.5m/s

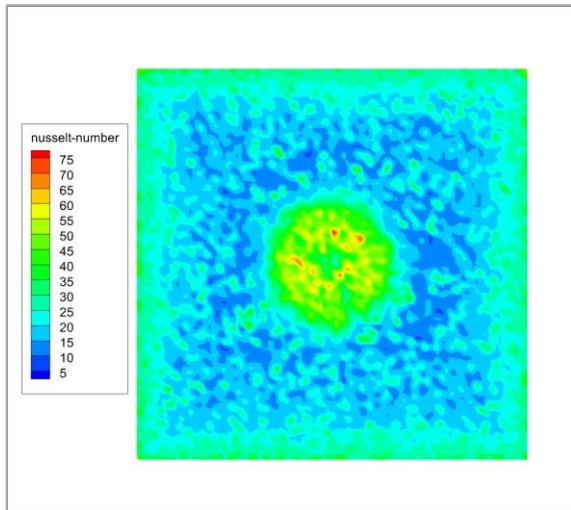


Figure 86 Nusselt no. at $n=1.2$ and velocity=1.5m/s

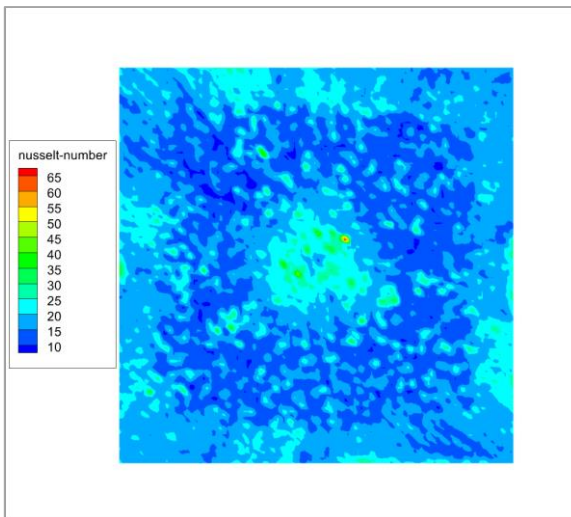


Figure 87 Nusselt no. at $n=1.4$ and velocity=1.5m/s

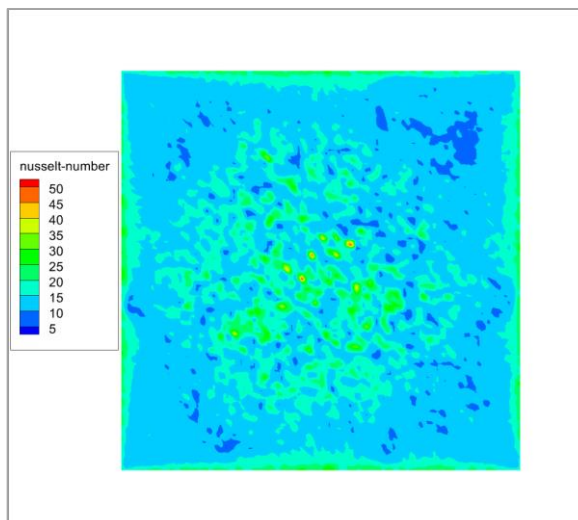


Figure 88 Nusselt no. at $n=1.6$ and velocity=1.5m/s

6.6 Temperature vs x coordinate variation chart plotted at the line drawn along the heated wall plate , for varying n, at velocity= 1.5m/s :

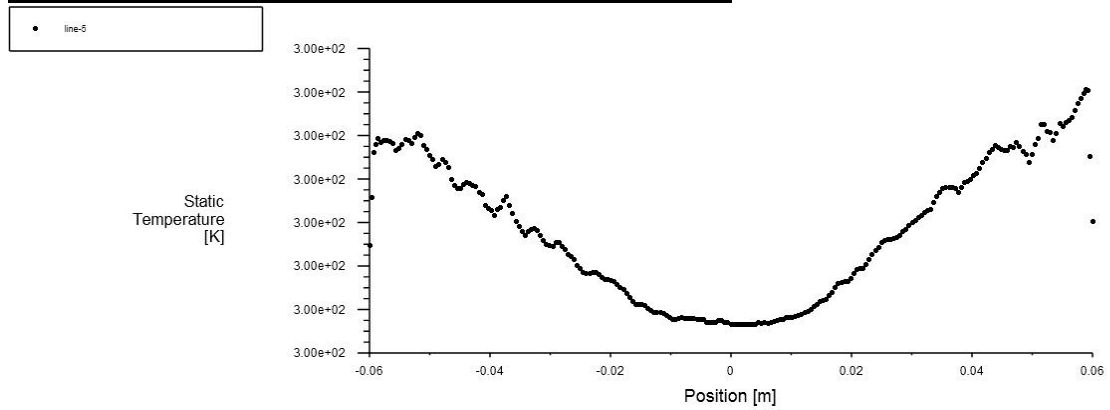


Figure 89 Temperature variation along line, at $n=0.6$ and velocity= 1.5m/s .

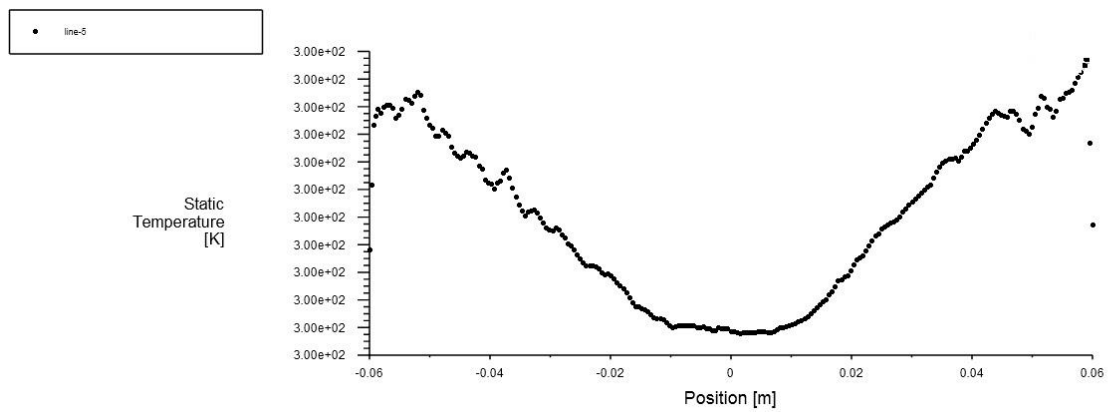


Figure 90 Temperature variation along line, at $n=0.8$ and velocity= 1.5m/s .

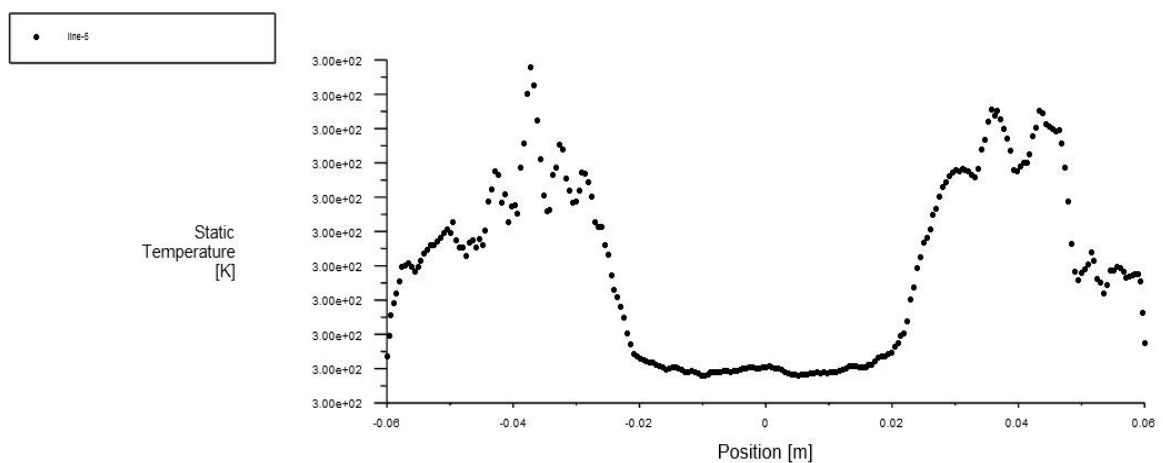


Figure 91 Temperature variation along line, at $n=1.0$ and velocity= 1.5m/s .

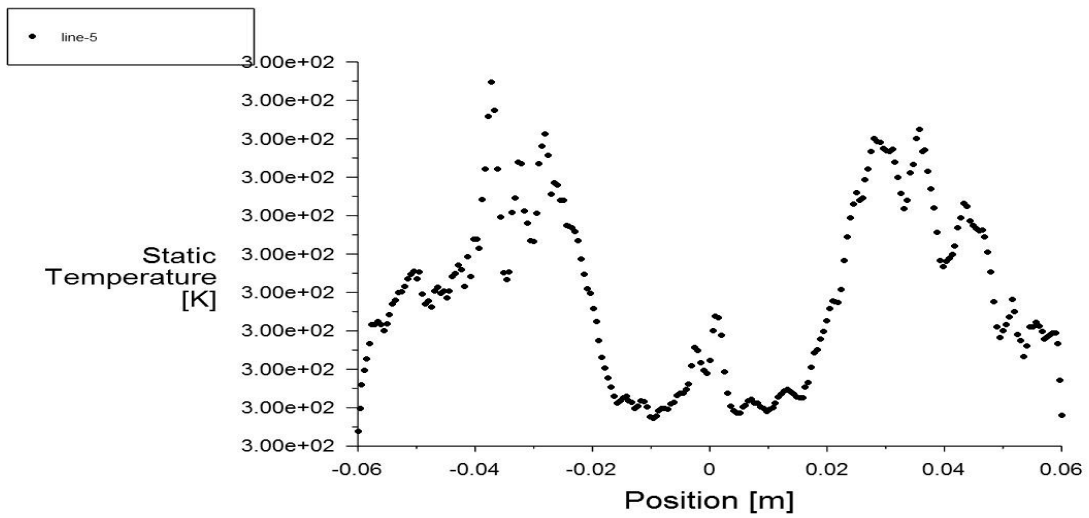


Figure 92 Temperature variation along line, at n=1.2 and velocity=1.5m/s.

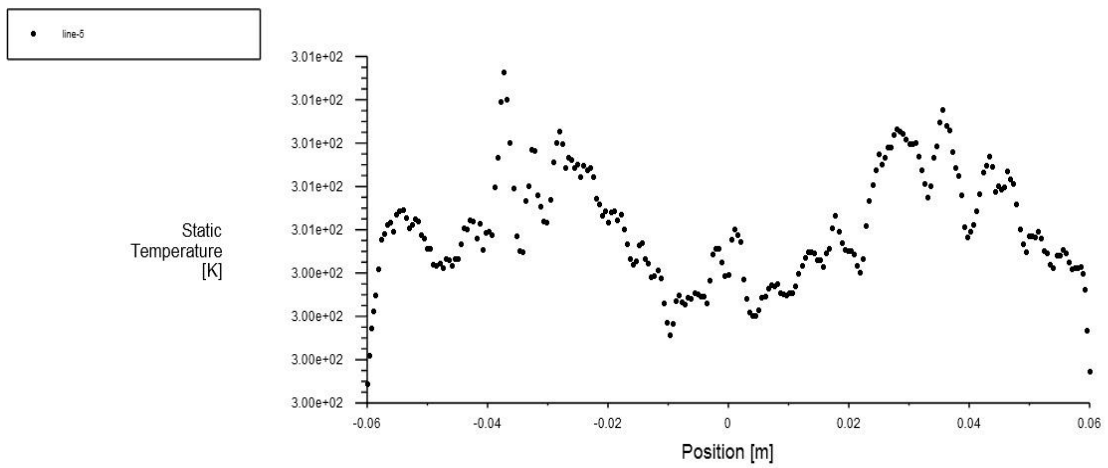


Figure 93 Temperature variation along line, at n=1.4 and velocity=1.5m/s.

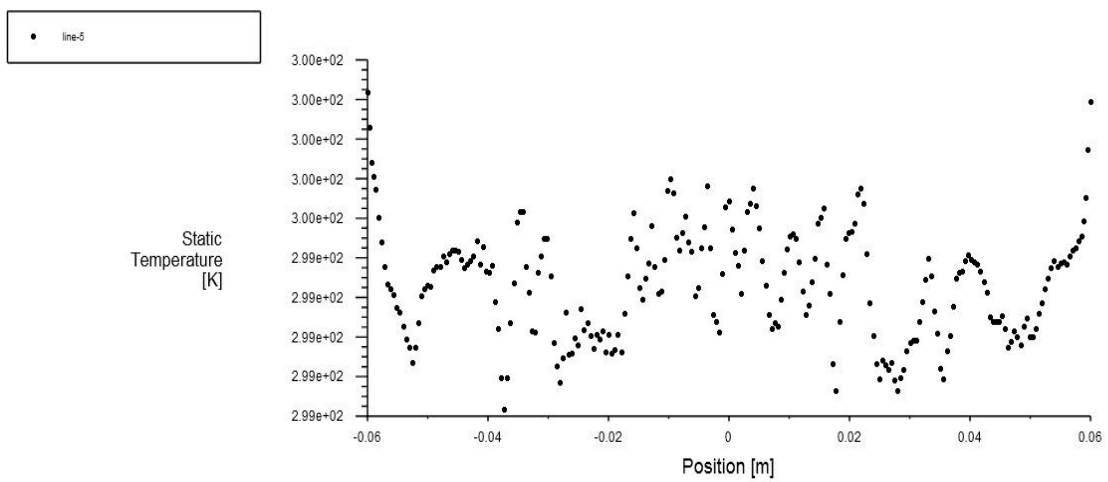


Figure 94 Temperature variation along line, at n=1.6 and velocity=1.5m/s.

6.7 Nusselt no. vs x coordinate variation chart plotted at the line drawn along the heated wall plate , for varying n, at velocity= 1.5m/s :

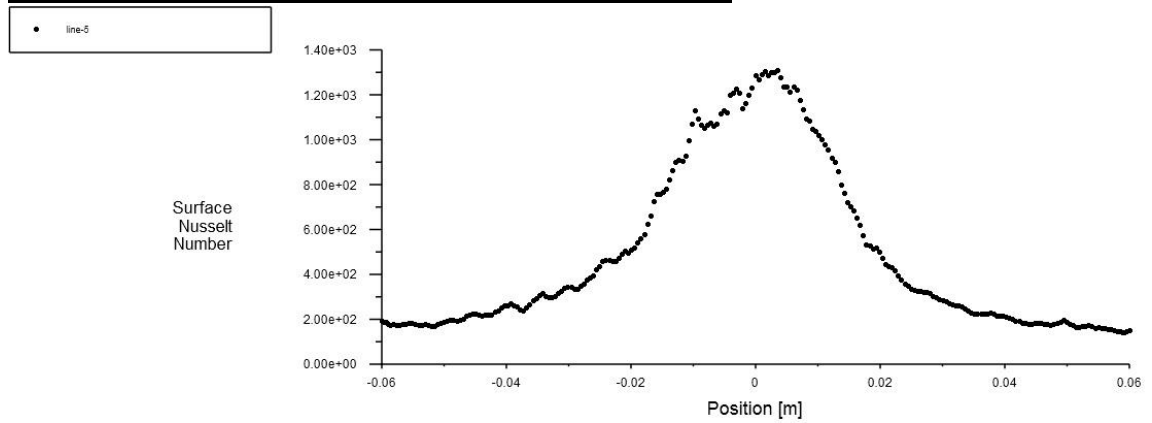


Figure 95 Nusselt no. variation along line, at $n=0.6$ and velocity= 1.5m/s .

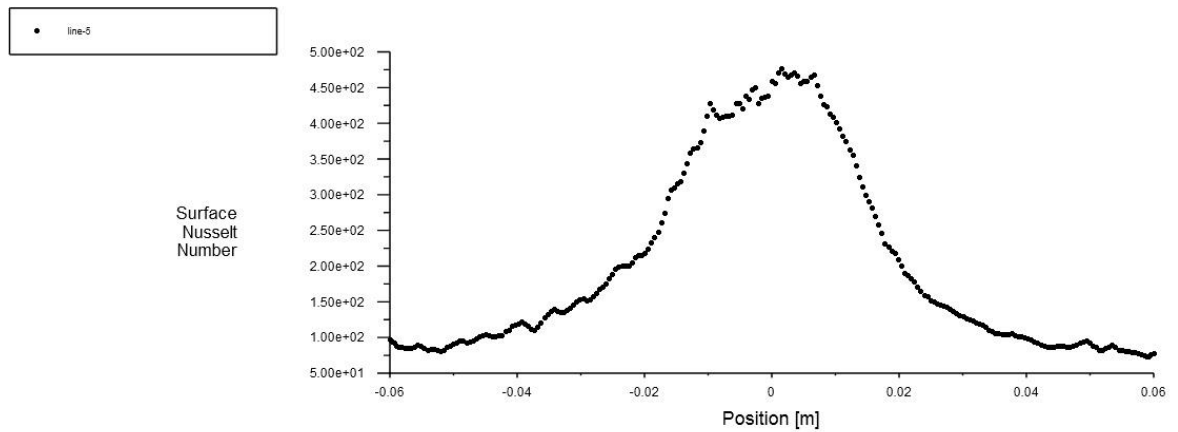


Figure 96 Nusselt no. variation along line, at $n=0.8$ and velocity= 1.5m/s .

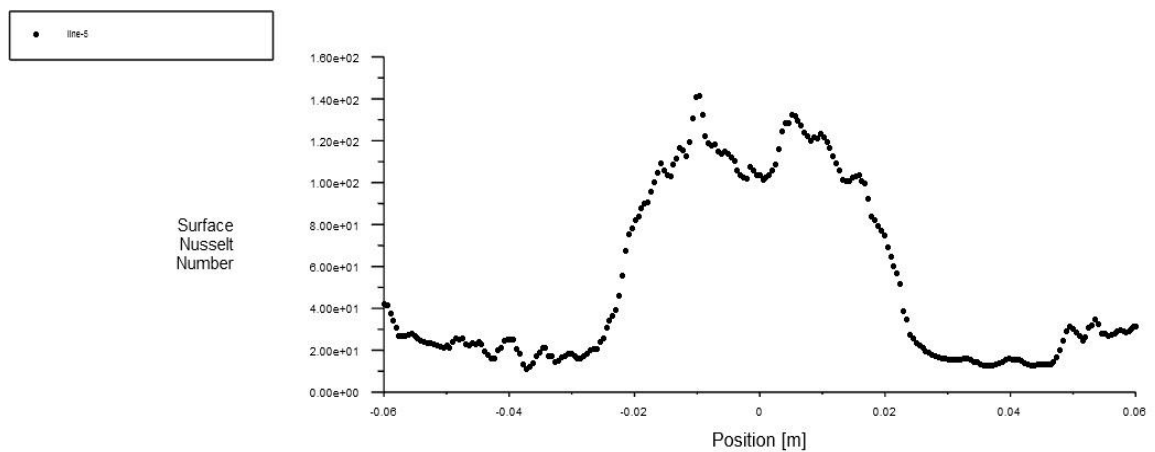


Figure 97 Nusselt no. variation along line, at $n=1.0$ and velocity= 1.5m/s .

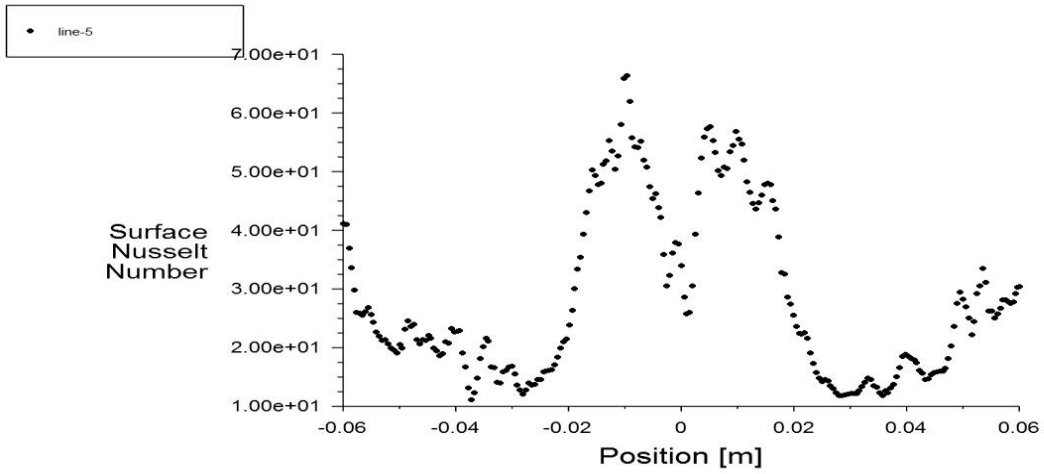


Figure 98 Nusselt no. variation along line, at $n=1.2$ and velocity=1.5m/s.

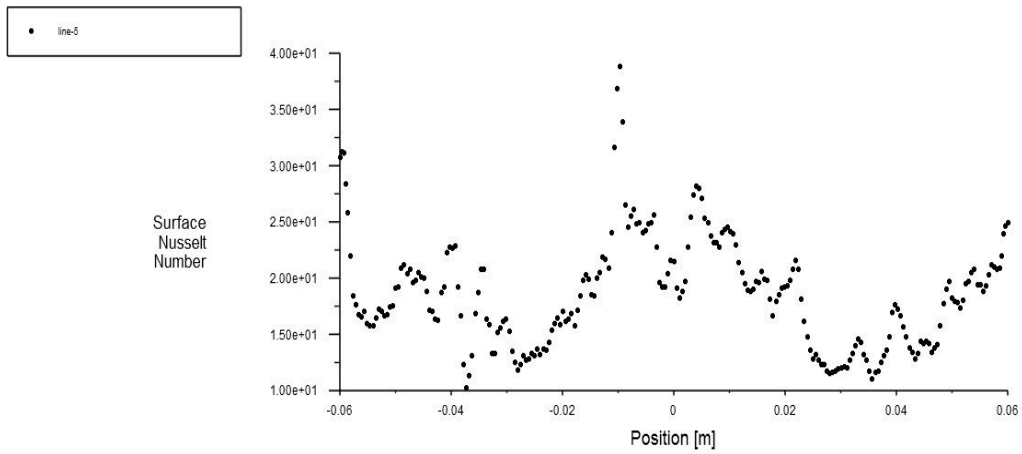


Figure 99 Nusselt no. variation along line, at $n=1.4$ and velocity=1.5m/s.

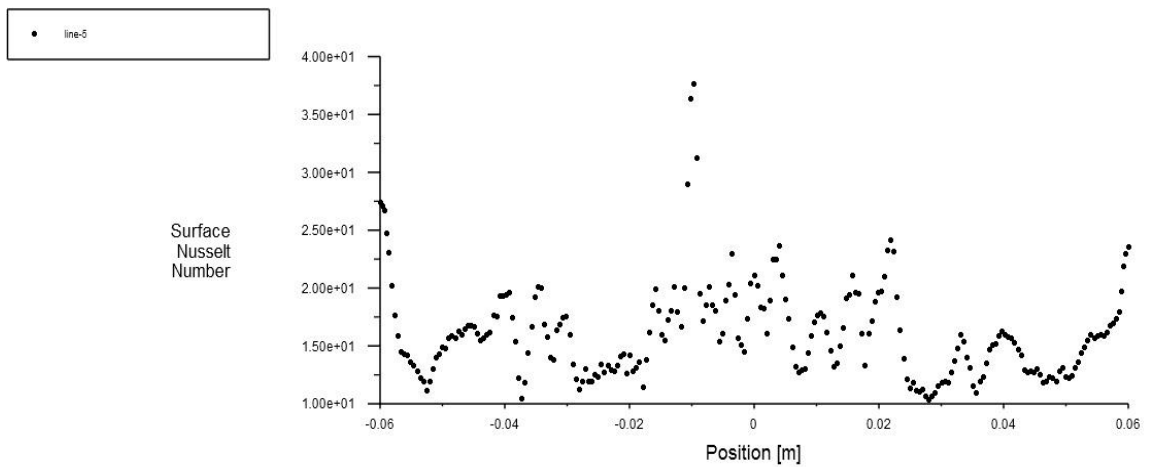


Figure 100 Nusselt no. variation along line, at $n=1.6$ and velocity=1.5m/s.

Conclusion

5.1 Conclusion

The present study dealt with the 3D simulation of the jet impingement on flat plate, where sinusoidal heat flux affected the temperature of the plate with time and corresponding heat transfer contours, Nusselt number and other parameters were observed and studied. Considering the power-law model, the results have been generated which described the cooling capacities of different fluids when impinged on the surface. The power-law index was gradually varied from 0.6 to 1.6 and the results were obtained for $v = 0.5$ m/s and 1.5 m/s. The results yield the following conclusions:

- The Pseudoplastic fluids (shear thinning fluids) shows better heat transfer characteristics comparing to Newtonian and Dilatant fluids.
- The difference in average temperature is very minimal for each cases, since the applied sinusoidal heat flux had low average value for the flow time and the thermal properties of fluid used had high values of specific heat as well as also thermal conductivity. The averaged heat flux value was calculated to be 841.47 W/m².
- Higher jet velocity provides better cooling performance. It can be seen from the Nu vs x/d plot drawn for both velocities.
- The core of jet gets thinner and shorter with increment in power law index.
- Position of the vortex formed gets farther away from the stagnation zone when velocity is increased. And vortex formation can be seen closer to the jet when power law index is increased.
- Average Nu number decreases with increment in the power law index, which shows better performance of shear thinning fluids in heat transfer rates.
- Better flowability of shear thinning fluids can be seen, in radial direction after the impingement.

- The stagnation zone has highest Nu no. and minimum Temperature values which shows maximum heat transfer occurrence in this zone, and it decreases in radial direction, showing poorer cooling in farther regions on the plate.

5.2 Future scope of this study

Newtonian fluid jets are less explored but can be good alternatives to for Newtonian fluids. The study shows the better heat transfer results for non-Newtonian Liquid Jet impingement, showing it as a good alternative for Newtonian fluids. Further study is required on this topic, with following variations:

- Study required for periodic heat flux impinging on different surfaces, flat, curved and periodic surfaces with effect of roughness.
- Single jet study has been performed in this work, it can be studied for multiple jets with non Newtonian fluids.
- A lot of study is required in the field of Impinging jets with varying temperature interacting with multiple fluids imping on different types of surfaces.
- Simulation studies along with the Experimental works with non-Newtonian fluids are required to be performed and analysed in detail.

The above stated scopes regarding this study can highly be helpful to understand, improve and achieve a better heat transfer characteristic, which will help in optimizing the crucial role of heat transfer, whether be it cooling or heating problems encountered in uncountable Industrial and general applications.

References :

- [1] R. Gharraei, A. Vejdani, S. Baheri, Numerical investigation on the fluid flow and heat transfer of non-Newtonian multiple impinging jets. *Int. J. Thermal Sciences*, (2016), Vol. 104, pp. 257–265.
- [2] Allauddin, Usman & Rehman, Naveed & Uddin, Naseem & Mahrukh, Mahrukh. (2018). Numerical Investigation of Heat Transfer by an Impinging Jet using Alumina-water Nanofluid. *Numerical Heat Transfer Applications*. 74. 10.1080/10407782.2018.1538293.
- [3] Ten, Jyi Sheuan Jason and Thomas Povey. “Self-Excited Fluidic Oscillators for Gas Turbines Cooling Enhancement: Experimental and Computational Study.” *Journal of Thermophysics and Heat Transfer* (2019): n. pag.
- [4] Y. C. Chen, C. F. Ma, and M. Qin, Theoretical Study on Impingement Heat Transfer with Single-Phase Free-Surface Slot Jets, *International Journal of Heat and Mass Transfer*, vol. 48. no. 16, pp. 3381-3386, 2005
- [5] M. Behnia, S. Parneix, and P. A. Durbin, Prediction of Heat in an Axisymmetric Turbulent Jet Impinging on Flat Plate. *Int. J. Heat and Mass Transfer*, (1998), Vol. 41, pp. 1845-1855.
- [6] Gus Nasif, Ram Balachandar & Ronald M. Barron (2016) CFD Analysis of Heat Transfer Due to Jet Impingement Onto a Heated Disc Bounded by a Cylindrical Wall, *Heat Transfer Engineering*, 37:17, 1507-1520.
- [7] X. Fuchang, S. Mohammed, Heat Transfer Behaviour in the Impingement Zone Under Circular Water Jet. *Int. J. Heat and Mass Transfer*, (2006), Vol. 49, pp. 3785-3799.
- [8] Teamah, M. A., Ibrahim, Dawood M. K. and Aleem M. M., 2012, "Experimental Investigation for Hydrodynamic Flow Due to Obliquely Free Circular Water Jet Impinging on Horizontal Flat Plate." *European Journal of Scientific Research* 83(1), pp. 60-75.
- [9] Bolek, Abdullah and Seyfettin Bayraktar. “Flow and heat transfer investigation of a circular jet issuing on different types of surfaces.” *Sadhana-academy Proceedings in Engineering Sciences* 44 (2019): 1-11.
- [10] K. Marzec and A. Kucaba-Pietal, Heat transfer characteristic of an impingement cooling system with different nozzle geometry, *IOP Journal of Physics: Conference Series* 530, 2014, 0122038

- [11] Sagot, Benoît et al. “Jet impingement heat transfer on a flat plate at a constant wall temperature.” *International Journal of Thermal Sciences* 47 (2008): 1610-1619.
- [12] Tahsini AM, Mousavi ST, Parametric Study of Confined Turbulent Impinging Slot Jets upon a Flat Plate, 6, 2012, 1220–1224
- [13] Liu, X. et al. “Convective Heat Transfer by Impingement of Circular Liquid Jets.” *Journal of Heat Transfer-transactions of The Asme* 113 (1991): 571-582.
- [14] Shang-Sheng Wu, Chin-Lin Shiu and Wen-Jyi Wu, “Analysis on transient heat transfer in a annular fins or various shapes with their bases subjected to a heat flux varying as a sinusoidal time function”, *Computers and Structures*, 61, (1996), 725-734
- [15] H. Martin, Heat and mass transfer between impinging gas jets and solid surfaces, in: j.p. hartnett, t.f. irvine (Eds.), *Adv. Heat Transfer*, Vol. 13, Academic Press, 1977, pp. 1–60.
- [16] S.J. Dovens, E.H. James, Jet Impingement Heat Transfer—A literature Survey, ASME paper 87-HT-35, 1987.
- [17] L.B.Y. Aldabbagh, A.A. Mohammad, Mixed convection in an impinging laminar single square jet, *ASME J. Heat Transf.* 131 (2009), 022201-1-7.
- [18] Tiwari et al. (2021). Turbulent Flow and Heat Transfer Characteristics of Non-Newtonian Impinging Jets on a Flat Plate. *Journal of The Institution of Engineers (India): Series C*. 102. 10.1007/s40032-021-00679-7.
- [19] J. Zhao, R.E. Khayat, Spread of a non-Newtonian liquid jet over a horizontal plate. *J. Fluid Mech.* 613, 411–443 (2008)
- [20] K. Zhu, P. Yu, N. Yuan, J. Ding, Transient heat transfer characteristics of array-jet impingement on high-temperature flat plate at low jet-to-plate distances. *Int. J. Heat Mass Transf.* 127, 413–425 (2018)
- [21] N. Saniei and X. Yan, Experimental study of heat transfer from a disk rotating in an infinite environment including heat transfer enhancement by jet impingement cooling, *Journal of Enhanced Heat Transfer*, vol. 7, no. 4, pp. 231 -245, 2000.
- [22] S.H. Seyedein, M. Hasan, A.S. Majumdar, Laminar flow and heat transfer from multiple impinging slot jets with an inclined confinement surface. *Int. J. Heat Mass Transf.* 37, 1867–1875 (1994)

- [23] H.J. Poh, K. Kumar, H.S. Chiang, A.S. Mujumdar, Heat transfer from a laminar impinging: jet of a power-law fluid. *Int..Commun. Heat Mass Transfer* 31, 241–249 (2004)
- [24] Y. Zhang, P. Li, Y. Xie, Numerical investigation of heat transfer characteristics of impinging synthetic jets with different waveforms. *Int. J. Heat Mass Transf.* 125, 1017–1027 (2018)
- [25] S. Caliskan, S. Baskaya, T. Calisir, Experimental and numerical investigation of geometry effects on multiple impinging air jets. *Int. J. Heat and Mass Transfer* 75, 685–703 (2014)
- [25] S. Caliskan, S. Baskaya, T. Calisir, Experimental and numerical investigation of geometry effects on multiple impinging air jets. *Int. J. Heat and Mass Transfer* 75, 685–703 (2014)
- [26] S. Hsieh, H. Tsai, and S. Chan, Local heat transfer in rotation square-ribroughened and south channels with jet impingement, *International Journal of Heat and Mass Transfer*, vol. 47, no. 12-13, pp. 2769-2784, 2004.
- [27] N. Saniei and X. Yan, Experimental study of heat transfer from a disk rotating in an infinite environment including heat transfer enhancement by jet impingement cooling, *Journal of Enhanced Heat Transfer*, vol. 7, no. 4, pp. 231 -245, 2000.
- [28] N. Zuckerman, and N. Lior, Jet Impingement Heat Transfer: Physics, Correlations, and Numerical Modeling, *Advances in Heat Transfer*, vol. 39, pp. 565-631, 2006.
- [29] Analytical Prediction of Thermal Behaviour during Cooling of a Hot Steel Strip, Shambhunath Barmana, Nilkanta Barmanb*, Achintya Mukhopadhyayc and Swarnendu Sen ,2017 Department of Mechanical Engineering, Jadavpur University, Kolkata, India
- [30] S. Inada, Y. Miyasaka, and R. Izumi, A Study on the Laminar Flow Between a Two-dimensional Water Jet and a Flat Surface with Constant Heat Flux, *Bulletin of the JSME*, vol. 24, no. 196, pp. 1803-1810, 1981.
- [31] X. S. Wang, Z. Dagan, and L. M. Jiji, Conjugate Heat Transfer between a Laminar Impinging Liquid Jet and a Solid Disk, *International Journal of Heat and Mass Transfer*, vol. 32, no. 11, pp. 2189-2197, 1989.

- [32] D. H. Lee, J. Song, and M. C. Jo, The Effects of Nozzle Diameter on Impinging Jet Heat Transfer and Fluid Flow, *Journal of Heat Transfer*, vol. 126, no. 4, pp. 554-557, 2004.
- [33] A. J. Bula, Numerical Modeling of Conjugate Heat Transfer During Impingement of Free Liquid Jet Issuing from a Slot Nozzle, *Numerical Heat Transfer, Part A: Applications*, vol. 38, no. 1, pp. 45-66, 2000.
- [34] D. H. Lee, J. Song, and M. C. Jo, The Effects of Nozzle Diameter on Impinging Jet Heat Transfer and Fluid Flow, *Journal of Heat Transfer*, vol. 126, no. 4, pp. 554-557, 2004.
- [35] V. Narayanan, J. Seyed-Yagoobi, and R. H. Page, An Experimental Study of Fluid Mechanics and Heat Transfer in an Impinging Slot Jet Flow, *International Journal of Heat and Mass Transfer*, vol. 47, no. 8-9, pp. 1827-1845, 2004.
- [36] Y. C. Chen, C. F. Ma, and M. Qin, Theoretical Study on Impingement Heat Transfer with Single-Phase Free-Surface Slot Jets, *International Journal of Heat and Mass Transfer*, vol. 48, no. 16, pp. 3381-3386, 2005.